Optimization of Heat Treatment process and Quenching cycles for Hadfield steel

Abdullah Alsebaie

2026

LUND UNIVERSITY

LTH
FACULTY OF ENGINEERING

MASTER THESIS

DIVISION OF PRODUCTION AND MATERIALS ENGINEERING

LUND UNIVERSITY

Supervisor: Mats Andersson

Industrial Supervisor: Latifa Melk, Material development expert Sandvik SRP AB

Examiner: Volodymyr Bushlya

Author: Abdullah Alsebaie

Lund, Sweden 2026

Avdelningen för Industriell Produktion

Lunds Tekniska Högskola

Lunds universitet

Box 118

221 00 Lund

Sverige

Division of Production and Materials Engineering

LTH, Faculty of Engineering

Lund University

Box 118

SE-221 00 Lund

Sweden

Printed in Sweden

Media-Tryck

Lund University

Foreword

This master's thesis was carried out in collaboration between the Division of Production and Materials Engineering at Lund University and Sandvik SRP AB in Svedala.

I would like to express my sincere gratitude to my industrial supervisor, Latifa Melk, for her continuous support throughout the thesis work and for providing the opportunity to carry out this project in an industrial environment. I would also like to thank Jörgen Petersson, Foundry specialist, and Henrik Göransson, Manufacturing Engineer, at Sandvik SRP for their valuable assistance in designing the experiments, meaningful discussions, and support throughout the project.

Special thanks also to Khalid Haddad, Material and Process Engineer, for his valuable insight and support during laboratory work and at the company. I am also grateful to all the personnel at Sandvik SRP AB who contributed during experimental work.

I would like to thank my academic supervisor, Mats Andersson, and examiner, Volodymyr Bushlya, for their guidance and valuable feedback throughout the thesis work.

Finally, I would like to thank my family for their continues support throughout my studies and especially during this project. Without their support, this work would not have been possible.

Lund 2026-05-25

Abdullah Alsebaie

Abstract

Hadfield steel is widely used in heavy-duty applications involving high impact loads and abrasive wear, such as mining and stone crushing equipment, due to its high toughness, ductility, and work-hardening ability. However, the as-cast microstructure contains carbide precipitation and chemical segregation, particularly along grain boundaries, which causes embrittlement and reduce service performance. Therefore, proper heat treatment followed by rapid quenching is essential to dissolve carbides and retain fully austenitic microstructure.

The aim of this thesis was to investigate and optimize heat treatment and quenching cycles for different Hadfield steel Grades, with focus on thermal gradients in thick sections, carbide dissolution, grain size, and hardness.

Two steel Grades were studied, GRADE A and GRADE B, using different sample geometries. Thick blocks were used to study thermal gradients between the core and surface, where plate samples were used to compare different heat treatment cycles.

The results showed significant differences between the surface and core temperature during the quenching, demonstrating the challenge of heat-treating thick Hadfield steel components due to the material's poor thermal conductivity. Among the heat treatment cycles investigated, the temperature step-down method prior to quenching and the two-step heat treatment showed promising results of carbide-free microstructure while maintaining refined grain size.

Overall, this thesis highlights the importance of optimizing the heat treatment and quenching parameters according to section thickness and chemical composition.

Keywords: Hadfield Steel, heat treatment, quenching, thermocouple.

Table of Content

1. Introduction

1.1.Background

In 1882, Sir Robert Hadfield discovered Manganese steel (i.e. Hadfield steel) which had remarkable properties of high toughness, ductility, high impact strength, and a unique ability of work-hardening. These characteristics made it an outstanding steel alloy option for heavy duties applications (e.g. Mining crushers, Railway tracks and armors). Hadfield steel is also non-magnetic steel. This type of steel has usually 1-1.2% Carbon, 10-14% Manganese, and it's usually combined with other alloying elements like Chromium, molybdenum, Nickel, Titanium, and Silicon. The manganese to carbon ratio is usually kept as 10:1 [1, 2].

Due to its high manganese content, Hadfield steel has an austenitic microstructure at room temperature, because the manganese delays the formation of martensite. The microstructure of the as-cast Hadfield steel is an austenitic microstructure with carbides segregating mostly on grain boundaries and inside grains. These carbides embrittle the steel, making it unsuitable for high-impact applications. To resolve this, the material must get a proper heat treatment under sufficient temperature and time to dissolve these carbides inside the matrix of austenite and then it must be quenched rapidly to freeze the alloying elements inside the matrix [3].

Sufficient heat treatment process is quite challenging, due to the poor thermal properties that this steel has, especially for large, thick parts such as stone crushers [4]. Industry leading companies like, Sandvik focus a lot on optimizing these processes to ensure a fully austenitic microstructure in their large cast parts.

This master's thesis will be conducted in collaboration with Sandvik SRP AB Svedala, and it will focus on optimizing the heat treatment process for Hadfield steel.

1.2. Aim and Objectives

The aim of this Master's thesis work is to investigate different heat treatment cycles and their effects on the microstructure and mechanical properties of the parts. Different heat treatment methods will be studied for different Hadfield steel alloys. Thermocouples will be implemented inside the parts to study the temperature homogeneity and temperature gradient between the core and the outer surface of the part during the heat treatment and quenching processes.

The main objectives of this project are:

- Monitor the temperature evolution during heat treatment using thermocouples placed at different depths.
- Evaluate different heat treatment and quenching cycles for various Grades of Hadfield steel.
- Study how does the different chemical compositions alter the microstructure and mechanical properties after the heat treatment.

1.3.Layout of the thesis project

In total there are five main sections in this report, it will start with a short introduction to help with understanding the problem that needs to be solved in this project. The second section will be the literature review to understand the relationship between chemical composition and their effects of the mechanical properties of the material, it will also include the different heat treatment processes and parameters to be able to determine the experiment to be conducted in this project. The third section will be the methodology used in this project, it will include the heat treatment processes parameters, the different Hadfield steel grades will be studied, the procedures and equipment will be used for both the experiment and the characterization process.

In the fourth section, the results and discussion will be stated and analyzed. Finally, a conclusion and recommendations for future work will be included in the fifth section.

2. Literature Survey

This chapter describes the theories that been found in the literature to build a foundation before performing experiments. It goes through the relationship between chemical composition and mechanical properties, what type of microstructure will be seen after and before heat treatment, and finally an investigation of different heat treatment methods and parameters.

2.1.Hadfield Steel

In 1882, Sir Robert Hadfield discovered Manganese steel (i.e. Hadfield steel) which had remarkable properties of like a high toughness level, high ductility, and high impact strength. This combination with its unique ability of work-hardening, make it an outstanding steel option for heavy duties applications (e.g. Mining crushers, Railway tracks and armors) [1, 2].

Hadfield steel has an austenitic FCC (Face Center Cubic) phase, which makes it highly ductile, it's also a non-magnetic steel. This type of steel has usually 1-1.2% Carbon, 10-14% Manganese and the manganese to carbon ratio is usually kept as 10:1. Different other elements are added to Hadfield steel to either enhance its properties [1, 2]. Changing the carbon or manganese content in Hadfield steel can have a huge effect on its mechanical properties and microstructure [5].

The microstructure of the as-cast Hadfield steel contains $(Fe, Mn)_3$ carbides segregating mostly on grain boundaries and inside grains. These carbides embrittle the steel, making it unsuitable for high-impact applications. To resolve this, the material must get a proper heat treatment under sufficient temperature and time to dissolve these carbides inside the matrix of austenite and then it must be quenched rapidly to freeze the alloying elements inside the matrix [3].

Hadfield steel has different standard Grades that range from 0.7% up to 1.45% of Carbon and from 6% up to 14% of Manganese [6]. These standard Grades are set by ASTM and are shown in the table below.

Table 1:Chemical Requirements for Austenitic Manganese Steel ASTM A128 [6].

Steel number		Composition (%wt)						
ASTM	UNS	C	Si	Mn	P	Cr	Ni	Mo
A	J91109	1.05~1.35	1.00 max	≥11.0	0.07 max	–	–	–
B-1	J91119	0.9~1.05	1.00 max	11.5~14.0	0.07 max	–	–	–
B-2	J91129	1.05~1.2	1.00 max	11.5~14.0	0.07 max	–	–	–
B-3	J91139	1.12~1.28	1.00 max	11.5~14.0	0.07 max	–	–	–
B-4	J91149	1.2~1.35	1.00 max	11.5~14.0	0.07 max	–	–	–
C	J91309	1.05~1.35	1.00 max	11.5~14.0	0.07 max	1.5~2.5	–	–
D	J91459	0.7~1.3	1.00 max	11.5~14.0	0.07 max	–	3.0~4.0	
E-1	J91249	0.7~1.3	1.00 max	11.5~14.0	0.07 max	–	–	0.9~1.2
E-2	J91339	1.05~1.45	1.00 max	11.5~14.0	0.07 max	–	–	1.8~2.1
F	J91340	1.05~1.35	1.00 max	6.0~8.0	0.07 max	–	–	0.9~1.2

When Hadfield steel is subjected to stress and impact loads, it undergoes plastic deformation, and the density of lattice dislocations start increasing rapidly. This increase in the dislocation makes further deformation harder, this phenomenon called work hardening. In Addition, another mechanism called twining occurs, which is a planner sliding defect that acts as additional barrier to dislocation motion. Both of these mechanisms increase the hardness and wear resistance of Hadfield steel during service, due to its supersaturated austenitic structure microstructure and low stacking fault energy (SFE) [7, 8].

Work hardening increases the hardness significantly, Hadfield steel has an initial hardness value between 190-220 HB, after Work hardening the hardness value can exceed 500 HB which is more than twice its initial value. In [8], the hardness of Hadfield steel was measured before and after service to assess the work hardening effects. The results showed a significant increase in the hardness values after service, it increased from 225HV5 to around 700 HV5 near the surface of the sample. The hardness of the sample's core didn't change after service, since work hardening affects only the outer surface [8].

2.1.1. Manganese Steel Phase Diagram:

Manganese Steel (i.e. Hadfield steel) consists of a fully Austenite (γ-Fe) microstructure which has a Face Centred Cubic (FCC) lattice. The As-cast microstructure could have some Manganese carbides in the grains and grain boundaries [5].

In a standard Iron-Carbon (Fe-C) phase diagram, Figure 1, Austenite phase exists between 738ºC - 1495ºC, which makes it impossible to obtain an austenitic structure in room temperature [9].

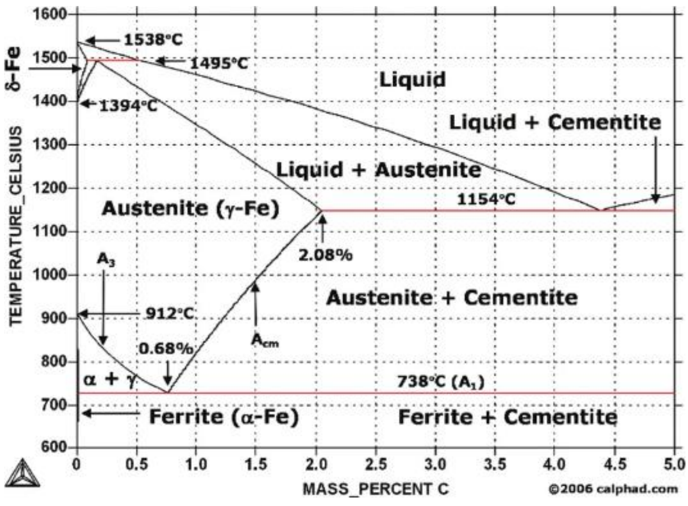

Figure 1: Fe-C Phase Diagram [9].

The addition of the alloying elements shifts the phase diagram and alters the thermodynamic behaviour of the steel phases the alloy. The high manganese content in Manganese Steel (i.e. Hadfield Steel) leads to austenite stabilizing which expand the austenite phase and make it possible to get a fully austenitic structure in room temperature.

The manganese addition effects are shown in Figure 2 and Figure 3, adding a 13% Manganese lowers down the bottom austenite temperature drastically to around 590 ºC and introduce the complex carbides $(Fe, Mn)_3C$ as M_3C in the diagram. Adding a 4.5% of Manganese doesn't change the austenite region much compared with plain steel, and it doesn't lead to austenite stabilization, but it still introduces the complex carbides [10].

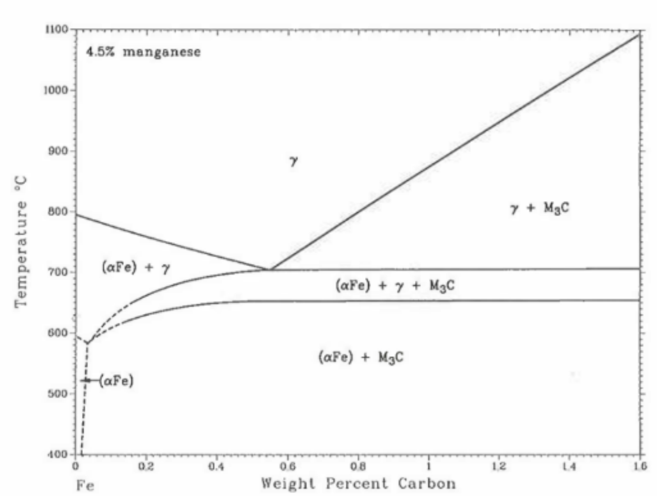

Figure 2: Fe-C-4.5Mn phase Diagram [10].

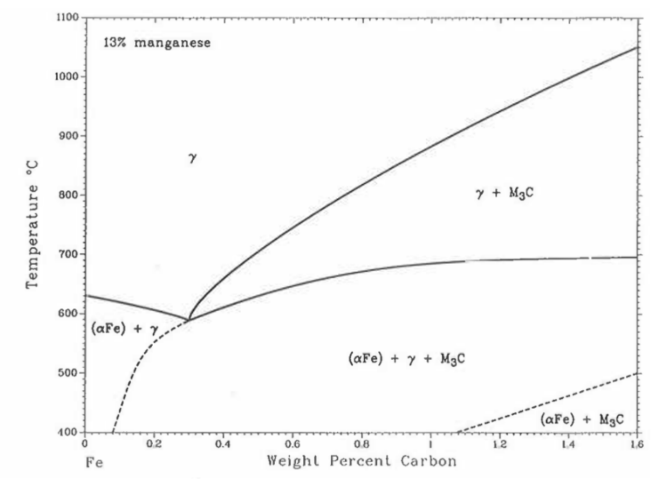

Figure 3: Fe-C-13Mn phase Diagram [10].

A typical Hadfield steel that has 13% Mn and 1.2% C, when it is slowly cooled it will have a microstructure consist of ferrite (α), Austenite (γ), Complex carbides

(M_3C) as seen from Figure 3 [10]. Only by proper heat treatment, a fully austenitic structure can be obtained [5].

2.2.Chemical Composition

To enhance the mechanical properties of Hadfield steel, the carbon and manganese content are changed or/and additional alloying elements are introduced to get special combination of properties according to the required application. Alloys like Chromium, Molybdenum, Nickel, Titanium, Aluminum, Silicon and others are added to obtain the desired properties [5].

The effects of the most used and presented alloying elements in Hadfield steel will be explained below:

2.2.1. Carbon

The carbon (C) content in Hadfield steel is considered one of the most important parameters due to its effect on both the mechanical properties and the microstructure of the part [4].

Increasing carbon content leads to enhance tensile strength, wear resistance, hardness, yield strength, while reducing elongation, toughness and impact resistance [4, 11, 12, 13].

On the other hand, carbon must be fully dissolved in the austenite matrix after the heat treatment process to avoid brittleness. Any increase in the part thickness will make it harder to dissolve all the carbon carbides, and this will lower the possible carbon content in big parts. Carbon decreases the melting temperature of Hadfield steel. Also, carbon content has a direct effect on the required austenitizing temperature and holding time; more carbon content will require more time and higher temperature. Carbon is the hardness driver in Hadfield steel, a higher carbon content increases both the hardness level and the hardenability of steel [4, 12, 11].

While the carbon content in standard Hadfield steel ranges between 0.7 - 1.4% Carbon, a 1% of carbon gives a high yield and tensile strengths. When the carbon content exceeds 1.2%, more carbides will be presented in the steel, these carbides precipitate on grain boundaries and causes embrittlement behavior in the steel, which reduces the toughness, ductility and impact resistance of the steel [4, 13, 12]. The effect of carbon content change on mechanical properties is shown in Figure 4.

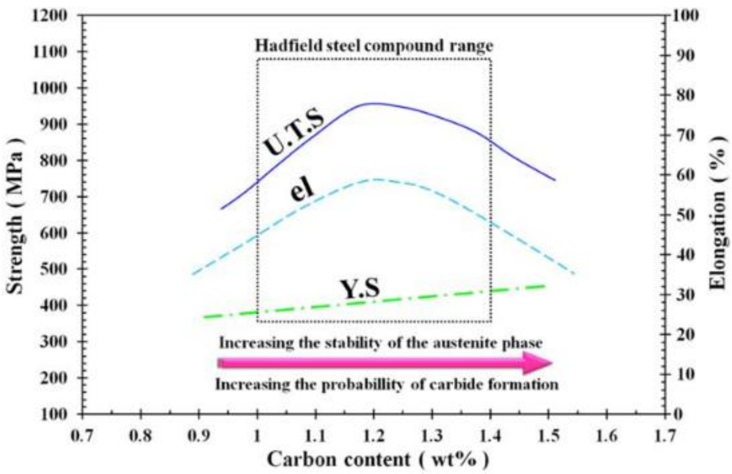

Figure 4: Carbon content effect on the mechanical properties [5].

2.2.2. Manganese

Manganese (Mn) is the star element of Hadfield steel because it's the reason why Hadfield steel has austenitic structure in room temperature. Manganese content in standard Hadfield steel ranges from 6 – 14%, and it affects both mechanical properties and the microstructure of the steel [3, 4].

Manganese acts as austenite stabilizer, it delays the cementite formation of steel which allows an austenite microstructure of Hadfield steel in room temperature. In other words, Manganese goal is to push the pearlite (Ferrite + Cementite) nose to the right in the Time-Temperature-Transformation (TTT) diagram to increase the cooling time range for austenite to stay in its microstructure [12, 13]. Manganese increases the solubility of carbon inside the Austenite matrix which allows more carbon content to a certain limit. It also increases the ductility and toughness levels, while reducing the Stacking fault energy (SFE) which increases the work hardening [13].

Increasing manganese content increases the number of carbides, specifically Mn_3C and $(Fe, Mn)_3C$ along grain boundaries. When the number carbides increase this leads to increase in hardness and yield strength up to certain level as shown in Figure 5. Increasing manganese to more than 14% makes the carbides much harder to control and makes them start clustering together which causes brittleness if they are not fully dissolve in proper heat treatment [5].

Furthermore, Manganese lowers the austenitizing temperature needed to dissolve the carbides and lowers the martensitic temperature (M_s) [4, 5].

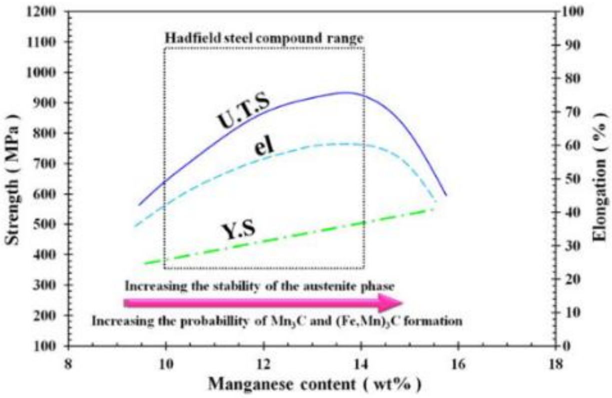

Figure 5: Manganese content effect on the mechanical properties [5].

2.2.3. Chromium

Chromium (Cr) is usually added between 1.5-2.5 % to Hadfield steel, to enhance the wear resistance and increases the hardness, yield strength and work hardening, but it has a negative effect to toughness [4, 12]. Chromium is a carbide forming element that forms big and complex carbides, such (Fe, Mn, Cr)$_{23}$C$_6$ and (Fe, Mn, Cr)$_3$C, these carbides improve the abrasive wear resistance but since they are complex carbides; achieving a fully austenitic structure after heat treatment becomes challenging, especially when Chromium content is increases over 2%, as seen in Figure 6 . [5, 14, 15]. Chromium is added to Hadfield steel to increase its initial yield strength which is relatively lower in standard Hadfield steel [5].

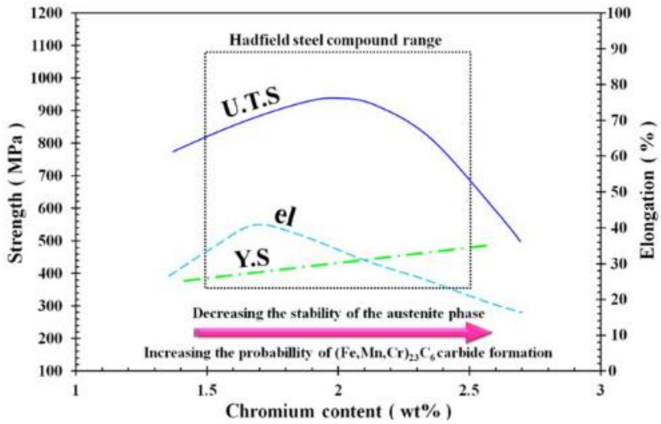

Figure 6: Chromium content effect on the mechanical properties [5].

2.2.4. Molybdenum

Molybdenum (Mo) is usually added between 1 - 2 % to Hadfield steel to increase the yield strength and tensile strength and unlike the other alloys it also improves toughness and ductility [4, 13]. Molybdenum has the ability to change the morphology of carbides; carbides usually form in long needle-like shapes along the grain boundaries which causes brittleness, but when Mo is added it forces the carbides to move inside the grains and form spherical-shaped carbides that make the steel tougher. Mo enhances also the as-cast mechanical properties, and it is mostly favorable added in big parts that have more than 6 inches thickness [16].

2.2.5. Aluminum

Aluminum (Al) is added to Hadfield steel to act as deoxidizer in very small amounts, usually 0.02-0.06 %; Adding more Al could lead to the formation of harmful inclusions. Additionally, Al helps to reduce the amount of carbides and changes their morphology into discontinuous form [5, 13].

2.2.6. Phosphorus

Phosphorus (P) is considered as impurity in Hadfield steel because of its harmful effects on the steel. ASTM A128, recommend that P content must not exceed 0.07% as shown in Table 1. Some papers even recommend that Phosphorus content should not exceed 0.04-0.05% [13, 14].

Phosphorus has a low solubility in solid austenite, when the casting solidifies the phosphorus get rejected outside grains to grain boundaries and forms Phosphide $(Fe, Mn)_3P$. The phosphide combines with Iron, Manganese, and carbon to form a triple phosphorus-carbide eutectic (Fe (Fe, Mn)3C (Fe, Mn)3P, this type of compound has a low melting point, and they melt during normal heat treatment process and then freeze during quenching along grain boundaries. This makes the Hadfield steel extremely brittle; thus, a low content of Phosphorus should be kept [14, 17].

2.2.7. Nickel

Nickel (Ni) is usually added to Hadfield steel to increase the machinability, especially weldability, and the ductility of the steel. Ni acts also as an austenite stabilizer, which can increase the wear resistance without forming carbides that could lower the ductility [13, 15] .

2.2.8. Silicon

Silicon (Si) is usually added to Hadfield steel in 0.5-1.5% to enhance the yield strength, hardness, and wear resistance without affecting negatively on the steel toughness if not it exceeds 1.4%. Si forms silicon particles (SiC) which increase hardness, and tensile strength as shown in Figure 7. Silicon can also prevent needle shaped carbides when added as 1% [5, 13].

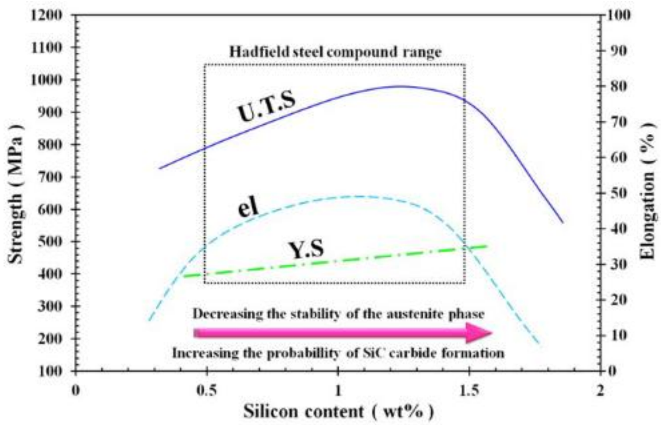

Figure 7: Silicon content effect on the mechanical properties [5].

2.2.9. Titanium

Titanium (Ti) is added to Hadfield steel in small amounts in the casting process as deoxidizer, but since it is a carbide forming element; it forms titanium carbides (TiC) which helps increasing the hardness, yield strength, wear resistance, while having a negative effect on toughness and impact resistance as shown in Figure 9 [5, 16]. A study showed that increasing the Titanium content to more than 0.4% has a small effect in enhancing the wear resistance of the steel, as shown below, but it lowers the impact strength dramatically. The sample with 0.4% Ti had an average impact strength result of 129 J/cm^2, while the sample with 2.5% Ti had only 57 J/cm^2 [18].

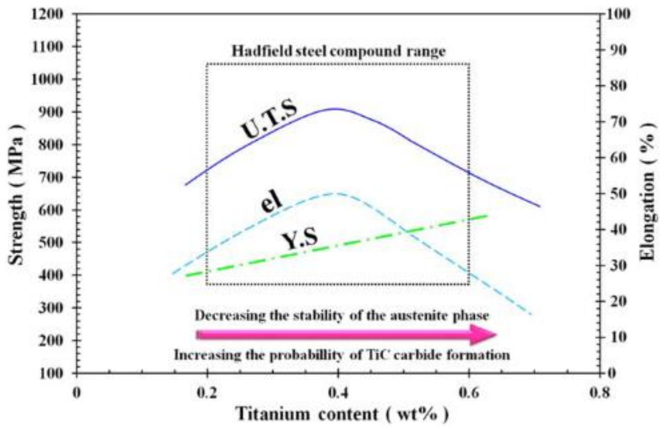

Figure 9: Titanium content effect on the mechanical properties [5].

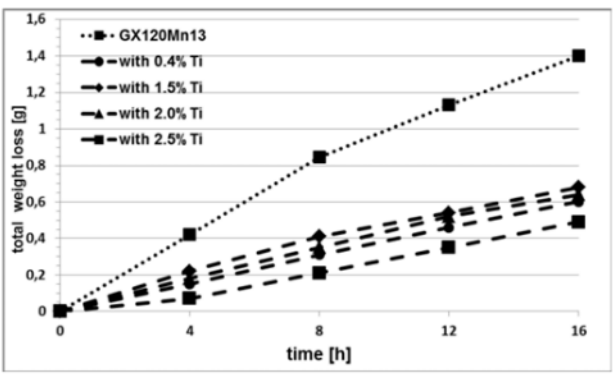

Figure 8: Total weight loss of samples over time [18].

2.3.Microstructure, Carbides, and Defects

The as-cast Hadfield steel has an austenitic microstructure matrix with carbides precipitating mostly in grain boundaries and slightly inside the grains. These carbides embrittle the material and make it fragile because they rais crack propagation. When Hadfield steel solidifies it forms a dendritic austenite structure and in the inter-dendritic spaces the remaining ferrite and cementite precipitate together with needle shaped manganese carbides $(Fe, Mn)_3$, as seen in Figure 10 and Figure 11 [19, 20].

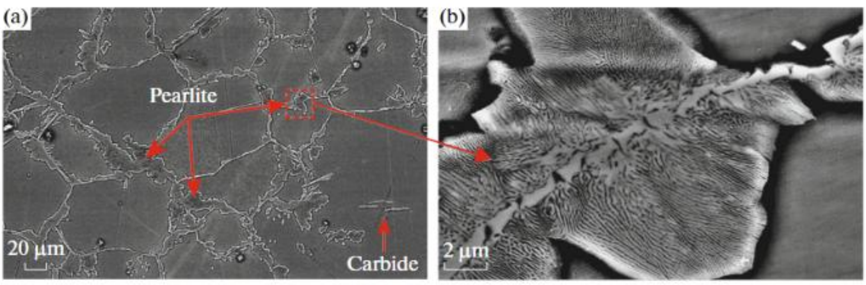

Figure 10: As-Cast Hadfield Steel SEM microstructure [19].

The As-cast microstructure happens due to the slow cooling (solidification) of the cast material. This condition of the material makes it unsuitable for most of the applications where Hadfield steel is usually used, due to its low toughness and brittle behavior. Thus, a proper heat treatment followed by rapid quenching must be made to dissolve the carbides in the matrix and form a supersaturated fully austenitic microstructure that have the desired properties of high toughness, high ductility, high wear resistance and work hardening [5, 14].

The difference in the microstructure between the as cast and heat-treated Hadfield steel is shown in Figure 12.

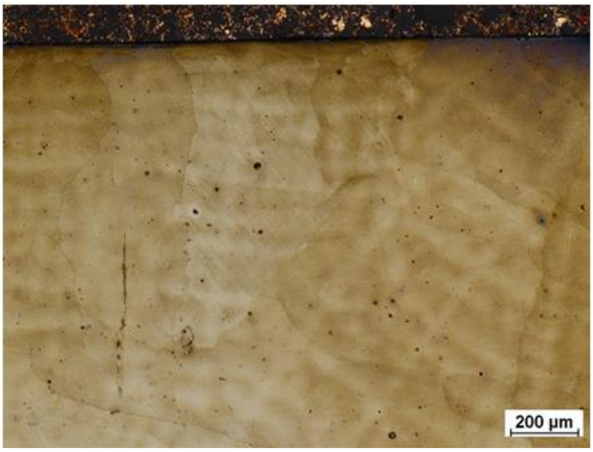

Figure 11: Dendritic structure in Hadfield Steel [8].

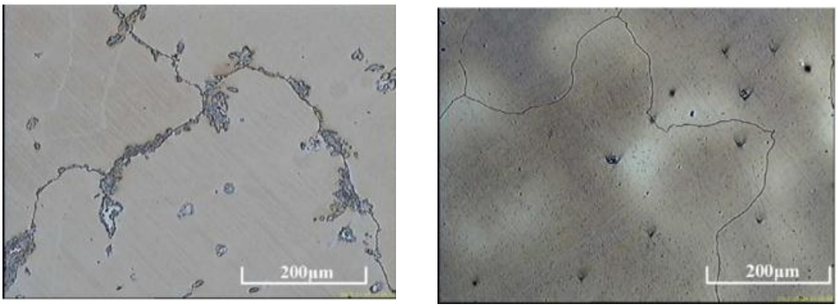

a b

Figure 12: Hadfield Steel: (a) before and (b) after Heat treatment [14].

Different types of carbides can form inside Hadfield steel; but the most common type is the alloyed cementite $(Fe, Mn)_3C$ type, which are presented in the as-cast condition of Hadfield steel, and number of carbides increases with the increase in the carbon content, especially when Carbon content is > 1.2% [19, 21].

Manganese carbides form due to the slow cooling process after casting, and they dissolve inside the austenitic matrix at around 1000-1100°C. Depending on the cooling rate of the quenching process they could reform in the steel microstructure [22].

The microstructure of manganese steel can be predicted from the cooling rate in the quenching process using the Time-Temperature-Transformation diagram (TTT). The TTT diagrams help in understanding the kinetics of isothermal transformation and when phase transformations begin and end [21, 22, 12].

As seen in Figure 13, the highest kinetic energy of carbides lays between the temperature range of 550 to 650° at the peak of the C-curve. There are two types of carbides that depend on their size [21].

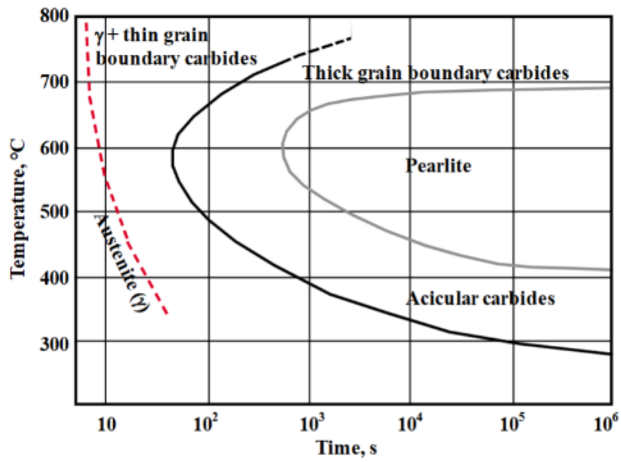

Figure 13: TTT diagram of 13%Mn and 1.2%C steel [21].

- Thin Carbides: which forms instantly during cooling, they have a thickness smaller than 0.2 µm. Thin carbides do not cause embrittlement to the steel and appear as fine separated particles along grain boundary lines under microscope. Thin carbides have a chemical composition very similar to the austenite matrix. They form first because they have a good lattice match with austenite, which makes them easier to nucleate at first, but since they are less thermodynamically stable; they don't grow [22].
- Thick Carbides: which form later and nucleate on thin carbides and grow along grain boundaries into continuous films causing a high embrittlement effect. Their initial thickness is usually in between 0.5 – 1.5 µm and usually have a richer chemical composition of Mn and other alloying elements compared to the austenite matrix. Thick carbides are more stable than thin carbides which makes them grow aggressively, but they take more time to form because of their higher energy interface with the austenite matrix [22].

In Figure 14, the arrow shows the transition from thin to thick carbides.

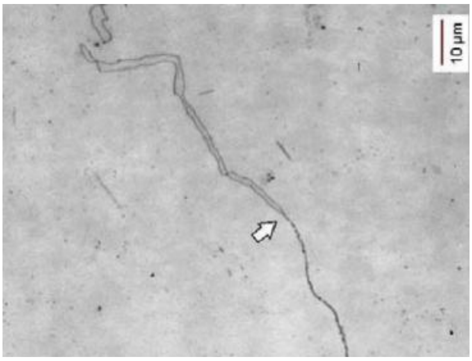

Figure 14: Thick carbides formation on thin carbides [22].

Other carbides can be presented in Hadfield steel depending on its chemical composition, many of the elements added to Hadfield steel are carbide forming elements such as Cr, Ti, V, etc., as explained in the 2.2 section.

Several other defects and embrittling phases can be present in Hadfield steel; the most common problems are explained as follows:

- Segregation: There are two types of segregation depending on their scale, they are macro-segregation and micro-segregation.
    - Macro-segregation occurs when the carbon and alloying elements concentrate more near the cast surface compared to the cast center, although its effects on the mechanical and thermal properties are negligible [22].
    - Micro-segregation, on the other hand, is when the alloying elements concentrate locally in inter-dendritic regions and grain boundaries which promotes the formation of harmful phases and carbides like the Phosphide-carbide eutectic which causes embrittlement as explained in 2.2.6 section above [14, 22].
- Microporosity: Microporosity is another common defect in Hadfield steel due to its long freezing range. The pores have very small and fine sizes, but their harmful effects increase because they tend to cluster within the inter-dendritic regions and grain boundaries which reduces the toughness of the casting [22]. Figure 15 shows intergranular microporosity.

- Shrinkage porosity: A special type of casting porosity is shrinkage porosity; it forms when the liquid steel starts solidifying and shrinking during feeding, which creates irregular cavities between dendritic spaces. It's observed in Hadfield steel as microporosity [23].

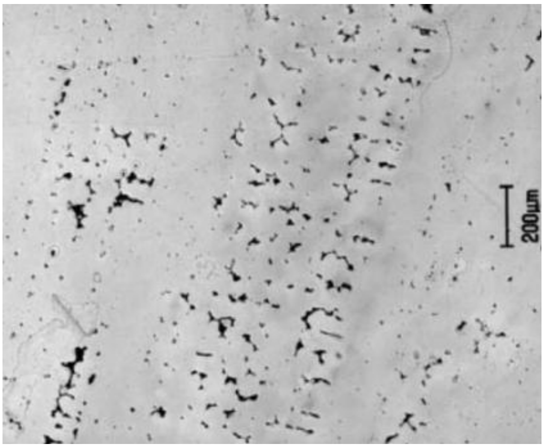

Figure 15: Microporosity in Hadfield steel [22].

2.4. Processing

The production of Hadfield steel components takes a long time because it involves several stages that have many details and are interdepend, making it a complex process. The main process flow consists of two stages:

I. Casting: The casting process starts with preparing the raw material that consists of manganese steel scrap and returns, with virgin alloying additions to achieve the required chemical composition of the selected Hadfield steel Grade. Sandvik AB, for example, uses up to 90% recycled material in their products as a part of their environmental agenda. The mix is put in an induction furnace and heated until it reaches around 1500°C and held at this temperature for a certain time to assure a proper chemical homogeneity. Before tapping the molten steel in the ladle, the chemical composition is checked, and the ladle is preheated to minimize heat loss. Deoxidizers like Al and Ti are then added to molten steel to remove excessive Oxygen and the slag is removed [4, 24].

Finally, the molten steel is poured into preprepared vacuum sand molds at around 1400°C and left to solidify and slowly cool [4].

II. Heat treatment: As explained earlier, the as-cast Manganese steel suffers from poor mechanical properties due to the precipitation of carbides during the slow cooling. Therefore, it must undergo through a proper heat treatment process to dissolve carbides and homogenize the microstructure. This treatment must be followed by a rapid quenching process to retain a fully austenitic structure at room temperature [5]. The heat treatment process will be further explained in the next section.

2.5. Heat Treatment and Quenching Principles

Most cast steels undergo heat treatment in order to improve their microstructure and properties, and Hadfield steel is no exception. The as-cast microstructure of Hadfield steel consists of coarse grains with carbides of the type $(Fe, Mn)_3C$ precipitating along grain boundaries and causing embrittlement behavior, as shown in Figure 12.

The objective of Heat treatment in Hadfield steel is to dissolve these harmful carbides, homogenize the microstructure, relieve internal stresses, and retain a single-phase fully austenitic matrix that has a high toughness and impact resistance [24].

2.5.1. Solution Heat Treatment

Hadfield steel undergoes solution heat treatment or solution annealing, which consists of ramping up the cast until it reaches the desired austenitizing temperature (usually around 1000-1100°C), held it at this temperature for a specified period, then quenching it rapidly. The standard used in the industry for the holding time is 1 hour per inch of section thickness plus 1 additional hour. For example, if the part is 6 inches thick; it should be held at the austenitizing temperature for approximately 7 hours [5].

Section thickness plays a huge role in the heat treatment process of Hadfield steel, due to its low thermal conductivity and poor heat transfer characteristics. When heat treating a very thick part (e.g., more than 4

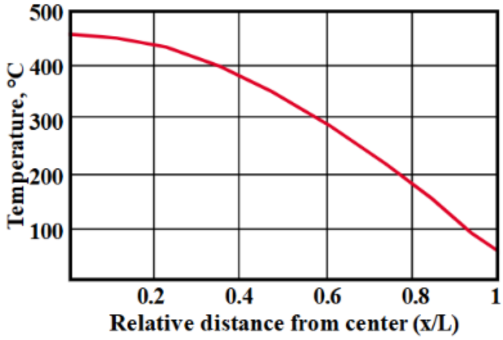

Figure 16: Thermal gradient of quenched Hadfield steel [21].

inches), the outside of the part (surface) will heat and cool much faster than the part's core. Figure 16, shows the predicted temperatures difference

across the cross-section of a block after quenching. The temperature may decrease and reach below 100°C on the surface, while staying above 400°C near the center of the part [21, 24].

This temperature gradient between the surface and core makes the outside layers of the part transform much faster than the inside layers near the core during quenching. If the gradient becomes large, it can lead to non-uniform thermal contraction, which increases residual stress and may potentially cause cracking. Additionally, large thermal gradients promote uneven grain growth and make it harder to remove existing micro-segregation, which affecting the performance of the final product [22, 24].

Hadfield thermal properties (e.g. specific heat) are temperature dependent, as shown in Figure 17. This reduces the accuracy of traditional tools such as Heisler charts, which assume constant thermal properties and are commonly used to analyze the thermal transfer within parts. A more

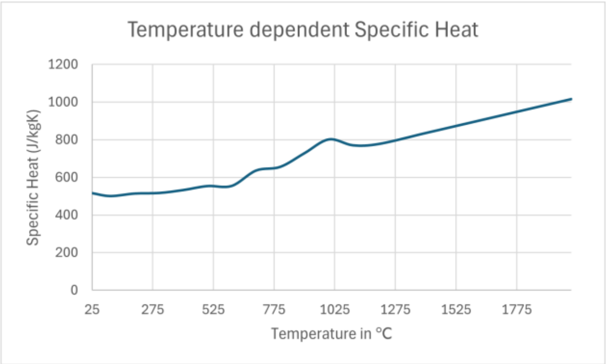

Figure 17: Temperature dependent Specific Heat of Hadfield steel [4].

appropriate way to study thermal gradients in thick parts is to implement thermocouples at different thicknesses inside the part during heat treatment, and to develop a simulation model that considers the temperature dependence of thermal properties of Hadfield steel. This accurate temperature measurement and proper modelling are essential to optimize the heat treatment process [4, 21].

2.5.1.1. Parameters affecting Heat treatment Process

- Austenitizing temperature: the maximum temperature that the part should reach during the heat treatment process. This temperature must be high enough to dissolve harmful carbides, and it can range from 950 to 1200°C depending on the chemical composition and geometry of the component. Higher austenitizing temperature generally results in greater carbides dissolution, higher yield strength, and hardness which are preferable. However, excessively high temperatures can also lead to grain growth which reduced ductility and fracture toughness [25].
- Holding time: the time for which the part is held at the selected austenitizing temperature in order to ensure temperature homogeneity throughout the section, ensure dissolving harmful carbides, improve chemical homogeneity between the core and surface of the part, and allow diffusion of alloying elements in the austenitic matrix. The holding time depends on the chemical composition, section thickness and the selected austenitizing

temperature; higher austenitizing temperature is often used to reduce the required holding time and shorten the total cycle time. However, if the part remains in the furnace after carbides dissolution is complete, grain growth will rise rapidly. The presence of carbides in the microstructure can help minimize grain growth by grain-boundary pinning effect, but once carbides are dissolved during heat treatment process, grain growth may accelerate rapidly, causing to a loss in the material toughness [24].

- Heating rate: the rate at which the part is heated to reach the desired austenitizing temperature. The heating rate is usually kept relatively low, around 100-200°C/hour, to minimize the thermal gradient through the part, which affect the risk of thermal stress and internal cracking [26, 27].

2.5.2. Quenching

After solution treatment has dissolved carbides and homogenized the alloying elements in the austenitic matrix, rapid quenching must be made to retain a fully austenitic and carbide-free structure. The final microstructure of the material is strongly influenced by the quenching rate. Hadfield steel is usually quenched in water at room temperature, and water agitation is necessary to achieve a rapid cooling and to control the water temperature, especially in industrial quenching tanks [5].

Quenching involves a heat balance relationship between the part, which loses heat, and the quenching water, which gains heat. Therefore, larger quenching tanks have greater heat extraction capacity [21].

Adding NaCl (i.e., Salt) at 1.5-3% to the quenching water can increase the cooling rates, which decreases the volume of carbides in the microstructure and improves material toughness. However, it could lead to surface cracking due to the very fast cooling at surface layers compared to core, which increases the thermal gradient and thermal stresses through the section, especially in materials that have poor thermal conductivity [28].

The cooling process during quenching has three main stages:

- Vapor blanket stage: when the part is immersed in water, a vapor blanket starts to form around the part. this vapor blanket acts as insulator, preventing direct contact between the water and the part surface. The cooling in this stage happens mainly by radiation, and the cooling rate is therefore relatively slow, which make this stage undesirable [21, 29]. Water agitation and salt addition can help in breaking the vapor blanket and reduce its duration [24].

- Nucleate boiling stage: once the temperature of the part surface drops, the vapor blanket breaks and the nucleate boiling stage starts. The quenching water starts touching the part directly, and intense boiling occurs. This stage has the highest cooling rates, is the most effective stage of quenching [21].

- Convective cooling stage: the final stage begins once the surface temperature of the part gets below the boiling point of the water, which stops the boiling. The quenching water then covers the part completely. The cooling rate in this stage decreases progressively, as the temperature difference between the part and the quenchant becomes smaller [21, 29].

Figure 18 presents a schematic representation of the heat-transfer coefficient as a function of time during the stages of quenching.

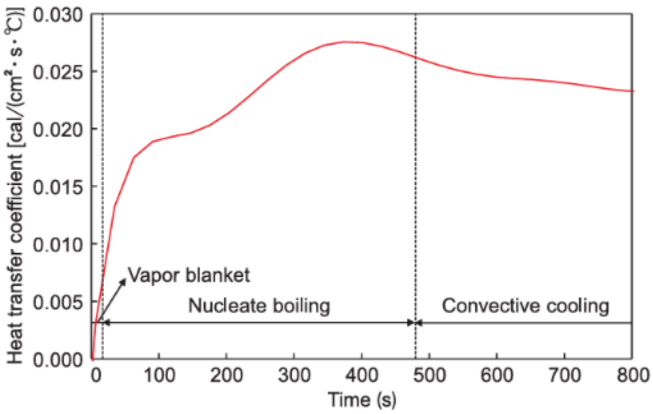

Figure 18:Heat-transfer coefficient during the three stages of quenching [29].

3. Methodology

This chapter describes the methodology used to carry out the experiments and analyses in this thesis. It begins by listing the materials studied in this thesis, followed by the heat treatment cycles investigated. It then presents the sample preparation procedures, followed by the equipment used for material characterization and, finally, the thermocouple setup used in this study. A schematic overview of the experimental procedure is shown below.

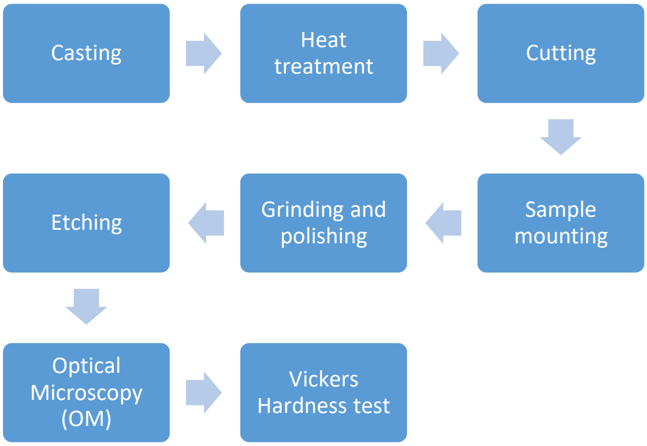

Figure 19: Overview of the Experimental procedure.

3.1. Materials

Two different Grades of Hadfield steel were studied in this thesis, with different chemical compositions to evaluate the effect of composition on the heat treatment process, in order to optimize it. Two different sample geometries were used for different investigations, as shown in Figure 20:

- 290*75*30mm (Length*Width*Thickness) plates: used to study different heat treatment and quenching cycles.
- 240*190*250mm (Length*Width*Thickness) block: used to study thermal gradient between core and surface.

Two Hadfield steel, Grades A and B, were selected for this study. Grade A represents a conventional Hadfield steel composition, similar to ASTM A128 Grade C, whereas Grade B contains higher levels of Mn and Cr. Grade B also contains grain refining elements, to act as nucleation sites and promotes finer grain structure, which is expected to increase the material toughness.

Additional alloying elements, including V, Ti, Al, Nb, were also present in both grades at low concentrations.

A) B)

Figure 20: Samples used in the experiments A) The block, B) The plate.

3.2. Heat Treatment Cycles

Different heat-treatment and quenching cycles were investigated to analyze their effects on carbide dissolution, grain sizes, and hardness levels. Five heat treatments were selected based on the literature survey and they were conducted on the selected steel Grades, as shown in Table 2.

No.	Heat treatment process	Sample Code
HT 1	Ramp heating to austenitizing temperature (6H) => Hold time (6H) => Water quench	A1 B1
HT 2	Ramp heating to austenitizing temperature (6H) => Hold time (1H) => Water quench	B2
HT 3	Ramp heating to austenitizing temperature (6H) => Hold time (1H) => step down to 1000°C (0.5H) => Water quench	B3
HT 4	Ramp heating to austenitizing temperature (6H) => Hold time (1H) => step down to 900°C (0.5H) => Water quench	B4
HT 5	Ramp heating to 700°C => Hold time (3H) => Ramp heating from 700°C to austenitizing temperature => Holding time (2H) => Water quench	A5 B5

Table 2: Selected Heat treatment Procedures.

The Heat treatment cycles are compared in Figure 21:

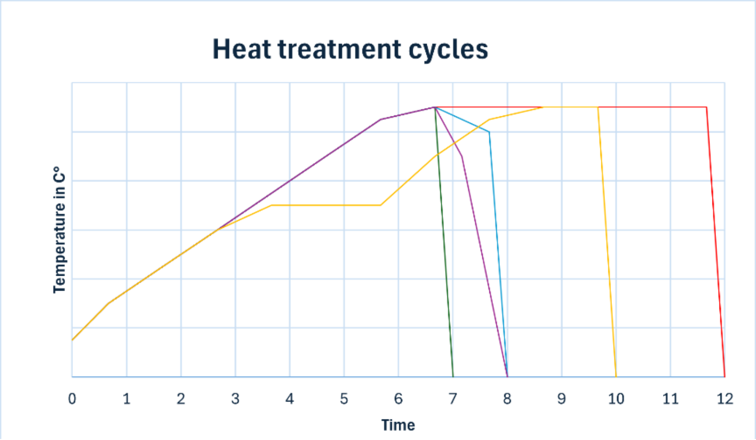

Figure 21: Selected Heat Treatment cycles.

3.2.1. Aim of selected heat treatment cycles

- **Heat treatment 1:** this cycle was selected to study the long heat-treatment program based on industrial heat-treatment practice for large parts. The blocks were used in this cycle, where they represent the thick-section products. Thermocouples were placed inside blocks at the core and near the surface, to get the thermal gradient, heating rate, and cooling rate, thereby evaluating the heat-treatment process. Additional thermocouple was put outside the blocks to study the atmosphere of the furnace during the heat treatment process and the water temperature during quenching.
- **Heat treatment 2:** this cycle was selected to study the industrial heat-treatment practice for smaller parts. The plates were used in this cycle and will be used as reference sample and compared with the other proposed heat-treatment cycles.
- **Heat treatment 3:** this cycle was selected to study the effects of stepping down the temperature of the furnace to 1000°C after the solution annealing stage, once carbides dissolution was assumed to be complete. The aim was to reduce the duration of the quenching process, thus potentially improving the effectiveness of quenching.
- **Heat treatment 4:** this cycle was selected to study the effects of stepping down the temperature of the furnace to 900°C after the solution annealing stage, once carbides dissolution was assumed to be complete. The aim was to reduce the duration of the quenching process and evaluate whether a lower pre-quenching temperature could improve the effectiveness of quenching.

- **Heat treatment 5:** this cycle was chosen to study the effects of two steps solution heat treatment on grain size. The aim was to investigate whether this heat-treatment cycle could refine the microstructure, thus improving the toughness and impact resistance of the material.

3.3. Sample Preparation

The different samples of plates and blocks were heat treated in car-type heat treatment furnace, as shown in figure 22.

Figure 22: Car-type industrial furnace.

After heat treatment, the plates were cut into small specimens for material characterization, using the cutter shown in Figure 23.

After cutting, the specimens were hot mounted in a *Struers-LaboPress-3* machine, to ease handling during grinding and polishing.

Figure 23: Saw cutting machine.

Figure 24: Example of a hot-mounted specimen.

The mounting parameters were 20 kN at 150 °C for 7 minutes, followed by cooling for 3 minutes. An example of a mounted specimen is shown in Figure 24.

The mounted samples were then ground and polished using a semi-automated *Struers-Tegramin-30* machine. The preparation program is listed below:

1. Piano 220: 25 N for 2 minutes and 40 seconds.
2. Piano 220: 20 N for 2 minutes and 40 seconds.
3. Allegro: 25 N for 3 minutes.
4. Allegro: 20 N for 3 minutes.
5. Dac: 25 N for 3 minutes.
6. Dac: 20 N for 3 minutes.
7. Nap: 20 N for 3 minutes.
8. Nap: 15 N for 3 minutes.

After polishing, a clear mirror-like surface was obtained. Nital etching was then carried out following the ASTM 407-07 standard to reveal the microstructure. A solution of 2% nitric acid in 98% ethanol was prepared, and a cotton swab was soaked in the mix and gently rubbed over the metallic surface for approximately 30 seconds. The specimens were then rinsed with ethanol, then dried using a hot air gun and covered to protect the surface until further analysis.

3.4. Material Characterization

The prepared specimens were examined using a Zeiss-Ax10 optical microscope to check grain size, grain morphology, and carbide precipitation within the microstructure. This analysis provides a general assessment of the microstructural changes from the different heat-treatment cycles.

After optical microscopy analysis, the average grain sizes were determined using the linear intercept method on four optical micrographs.

Finally, Vickers hardness testing was performed using a manual *Struers Duramin* hardness tester. A matrix method was applied using a test load of HV1 (9.807 N) and a dwell time of 9 seconds. Eight indents were made in a 4 x 2 matrix at the center of each specimen, as shown in Figure 26. The average hardness value for each specimen was calculated and used to compare the effect of the heat-treatment cycles on the hardness of the material.

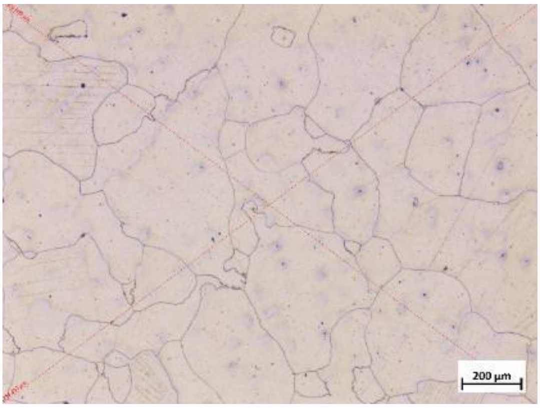

Figure 25: Linear intercept method to determine grain sizes.

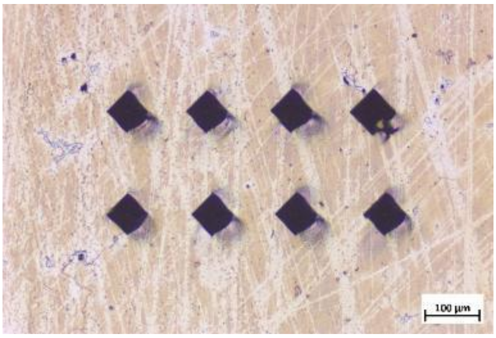

Figure 26: Indentation matrix pattern for the hardness testing at the center of specimen.

3.5. Thermocouples

K-type thermocouples connected to a Novus field logger were used in the experiment in this thesis to obtain the thermal gradient values during the heat treatment and quenching processes.

As described in Heat Treatment 1, thermocouples were placed into high manganese steel blocks at different depths to measure the heating and cooling rates during the heat treatment and quenching processes. This helps in determining the thermal gradient between the core and the region near the surface of the block.

Figure 27: Thermocouples experimental setup.

For this experiment, the blocks were first cast, then the riser was removed and a handle was welded onto each block to ease the handling of the block. The blocks were then sent to a machining center to drill two holes with a Ø of 10.2 mm, at different depths to measure both the core temperature and near surface temperature.

After drilling, ceramic tubes were used to position the thermocouples inside the holes and reduce the hole diameter. Thermocouples were then inserted and fixed using a temperature-resistant cement to seal the gap and prevent the quenching water from coming into direct contact with the thermocouples. This ensured that the recorded temperature is the temperature of the metal rather than the water.

4. Results and Discussion

This chapter presents and discusses the results obtained from the different experiments and heat treatment investigated in this thesis. The effects of the various methods of heat treatment cycles on the microstructure and mechanical properties of the Hadfield steel will be evaluated.

4.1. Thermocouples

After the installation of the thermocouples inside the two blocks, they were placed on a special fixture and placed inside a car type furnace. A 12-hour heat treatment cycle consisting of 6 hours of ramping up steps and 6 hours of holding time at austenitizing temperature was run on the blocks, followed by water quenching to capture the heating and cooling behaviors.

Figure 28: Taking out the blocks from the furnace.

Figure 30: Moving the blocks to the quenching pool.

Figure 29: Blocks quenching

The experiment was successfully completed, and the heating and cooling data were recorded using the data logger and exported to Excel for analysis.

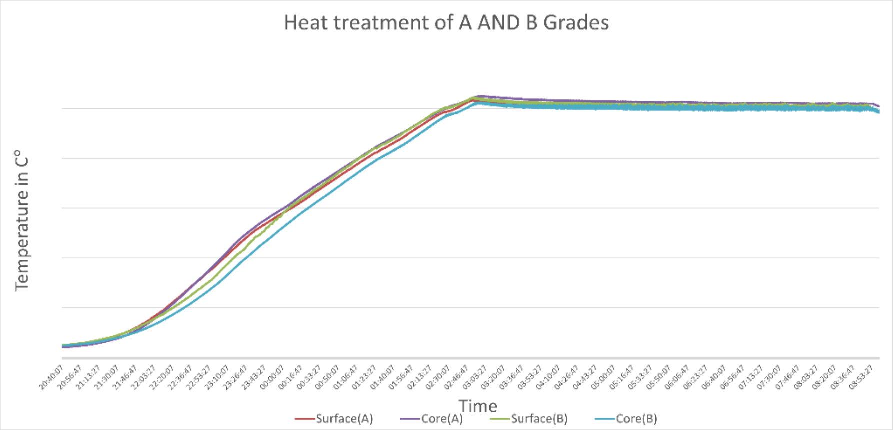

Figure 31: Heating rates of both steel Grades.

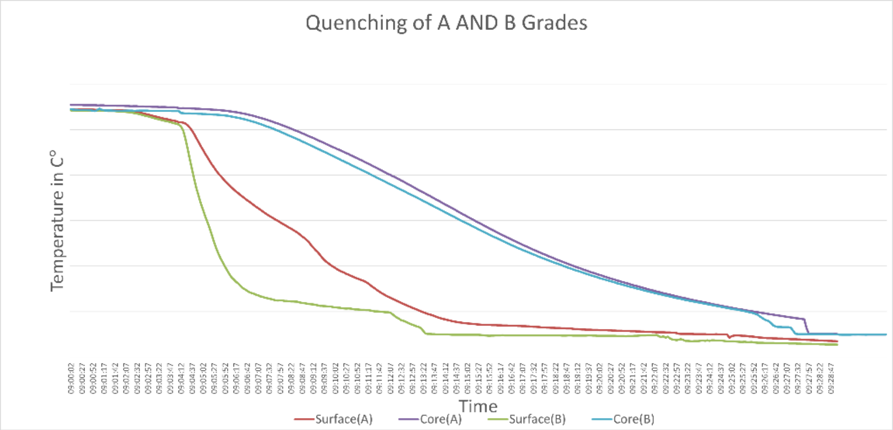

Figure 32: Cooling rates of both Grades.

As shown in Figure 31, the temperature evolution during the 12 hours heat treatment cycle was successfully captured. For the grade B block, the temperature measured by the near surface thermocouple showed a lower temperature than the core with an average temperature difference of around **15-35°C**, the surface reached the austenitizing temperature after approximately **30-50 minutes**, and it took the core additional **10-30 minutes** to reach the same temperature.

In the grade A block, a different trend was observed, the temperature of the near surface thermocouple showed a lower temperature than the core with an average temperature difference of around **5-25°C**, the surface temperature reached the core temperature in approximately **5-30 minutes**.

Overall, both steel grades reached similar temperatures levels at the same time which suggests that the difference in the chemical composition did not significantly influence the thermal conductivity under the tested conditions. Additional details are explained in Table 3.

Comparison points	**Average Value difference**
GRADE A(Surface) – GRADE A(Core)	5-25 °C
GRADE B(Surface) – GRADE B(Core)	15-35°C
GRADE A(Surface) – GRADE A(Core) to austenitizing temp.	5-30 minutes
GRADE B(Surface) – GRADE B(Core) to austenizing temp.	30-50 minutes

Table 3: Temperature differences during heat treatment.

After the completion of the heat treatment cycle, the blocks were quenched and the cooling rates were recorded, as shown in Figure 32. For the grade B block, the near surface temperature drops dramatically upon immersion in water, reaching a temperature below 200°C in **5-25 minutes**. This temperature is considered sufficiently low to prevent carbide precipitation. In contrast, the core took around **25-35 minutes** to reach the same temperature.

In the grade A block, a similar cooling trend was observed, although the surface cooling rate was slightly lower than that in the grade B block. The near surface temperature reached a temperature below 200°C, within **10-25 minutes**, while the core temperature required approximately the same duration to the grade B block to cool down. Additional details are explained in Table 4.

Comparison points	**Average Value difference**
GRADE A(Surface) – GRADE A(Core)	200-300°C
GRADE B(Surface) – GRADE B(Core)	300-400°C
Water temperature – GRADE A(Core)	500-600°C
Water temperature – GRADE A(Surface)	200-300 °C
Water temperature – GRADE B(Core)	500-600°C
Water temperature – GRADE B(Surface)	100-200 °C
GRADE A(Surface) to 200°C	10-25 Minutes
GRADE B(Surface) to 200°C	5-25 Minutes
GRADE A(Core) to 200°C	25-35 Minutes
GRADE B(Core) to 200°C	25-35 Minutes

Table 4:Temperature differences during quenching.

During the heating stage of the grade A block, an unusual temperature trend was observed, where the thermocouple located at the core showed higher temperature readings compared to the thermocouple near the surface. This behavior was not expected, as the heat transfer should occur from the furnace environment to the surface then to the core. This variation is most likely a thermocouple installation issue. During the installation of the ceramic tubes inside the drilled holes, dimensional tolerances caused fitting problems. One of the holes in the grade A block was slightly smaller than the 10.2 mm diameter, which made the 10 mm ceramic tube hard to insert inside the hole. To solve that, a smaller ceramic tube of 6 mm was used and inserted instead. This configuration likely caused radiation shadowing effects, that altered the core temperature readings in the grade A block. Nonetheless, the smaller tube didn't cause any problem in the quenching process, and the readings remained stable and reasonable for all the thermocouples.

The captured heating and cooling curves provide valuable insight into the heat treatment process. The applied heat treatment method had an approximately 100-200°C/h heating rate in the ramping up stage, resulting a low thermal gradient which didn't cause any thermal stress. This suggests that a higher heating rate, such as 200-300°C/h, could be potentially used to reduces the ramping up stage duration from 6 hours to approximately 5 hours, thereby improving process efficiency and reducing energy consumption.

The captured cooling rates during quenching indicate that the near surface region were quenched rapidly, demonstrating effective heat extraction and sufficient water agitation. However, the main limitation lies in the slow heat transfer from the core to the surface, which delays the cooling of the core region. This limitation is primarily related to the poor thermal properties of Hadfield steel rather than the quenching process itself, which highlights the difficulty of quenching parts with large section thickness.

Additionally, the transfer time from the furnace to the quenching bath was longer than in typical industrial practices due to the presence of the thermocouples and wires. The transfer took more time in this experiment and during transfer, the near surface temperature decreased by around 60°C and the core temperature only decreased by 15°C.

4.2. Optical Microscopy

Optical microscopy was used to examine the microstructure of the different steel grades and to evaluate the effects of the various heat treatment cycles on grain boundaries and carbide precipitation, particularly at grain boundaries.

4.2.1. Grade A:

The grade A manganese steel includes several conditions, starting with as-cast state.

I. As cast grade A

The as-cast grade A microstructure shows a high level of carbide precipitation both along grain boundaries and within grain, as shown in Figure 33.

The microstructure consists of coarse-grained austenitic matrix with is consistent with the expectation based on the literature. Several particles are observed precipitating along grain boundaries and inside grains. These particles are most likely alloyed Carbides, formed due to segregation of carbon and alloying elements such as Manganese and Chromium during solidification. These carbides will act as stress concentration sites and potentially initial cracking points, leading to embrittlement and reducing the service performance of the material.

In addition, several irregular dark features are observed near grain boundaries, which may represent shrinkage porosities, a common casting defect.

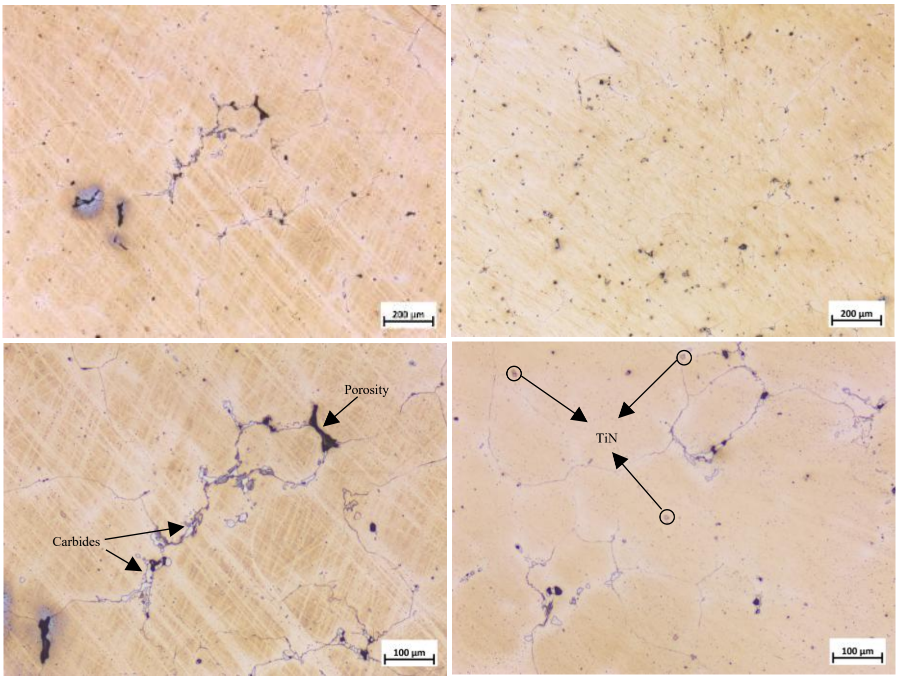

Figure 33: As cast grade A Microstructure.

Small particles are observed over the sample; these particles are most likely Titanium Nitrides (TiN) based on their golden appearance. however, these features require confirmation through SEM/EDS analysis.

These observation highlights the importance of proper heat treatment to dissolve carbides into the austenitic matrix and to improve the chemical homogeneity within the material.

II. HT1- X (GRADE A1)

Heat treatment 1 represents a long heat treatment cycle of 12 hours, consists of 6 hours ramping up and 6 hours holding time, and is typically applied for larger parts with section thickness above 140 mm. Due to the thickness of the block, samples were taken from different depths as shown in Figure 34.

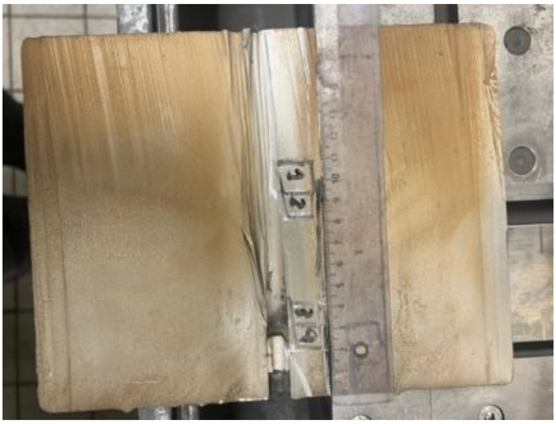

Figure 34: Grade A1 samples location

Three different regions were analyzed:

- At the edge of the block:

The edge represents the region in the block with the longest exposure to solution-treatment and the fastest cooling rate during quenching.

The microstructure consists of coarse-grained austenitic matrix and mostly clean grain boundaries. Carbide precipitation along grain boundaries is significantly reduced compared to the as-cast condition, indicating that the heat treatment was effective in dissolving most of carbides and that the rapid quenching limited carbide re-precipitation.

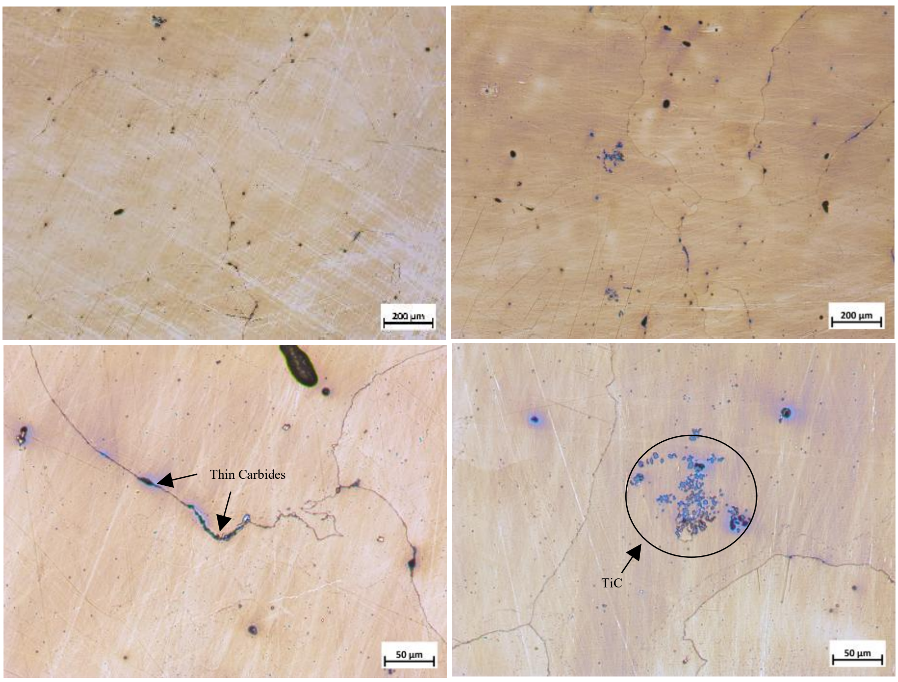

Figure 35: Grade A1-Edge Microstructure.

Most of the as cast carbides network appears to be dissolved, although thin features are still observed along some grain boundaries. These are likely undissolved alloy carbides; however, their limited presence will not affect the mechanical performance of the material.

In addition, agglomerates of small cubic dark particles are observed within the grains. Based on their morphology and contrast, these particles are most likely Titanium Carbides (TiC). Further confirmation through SEM/EDS analysis is required.

- Near the surface of the block:

This region represents 1 inch depth from the surface which experienced slightly shorter soaking time and a slower cooling rate compared to the edge.

The microstructure consists of an austenitic matrix with small particles along the grain boundaries; these particles are most likely re-precipitated carbides. Although these carbides are present, they are not continuous throughout the sample, which suggests that the heat treatment was effective in dissolving most of the carbides.

The bright particle observed inside one grain may be an alloy-rich carbide of a heavy element like Chromium, but this needs to be confirmed using SEM/EDS.

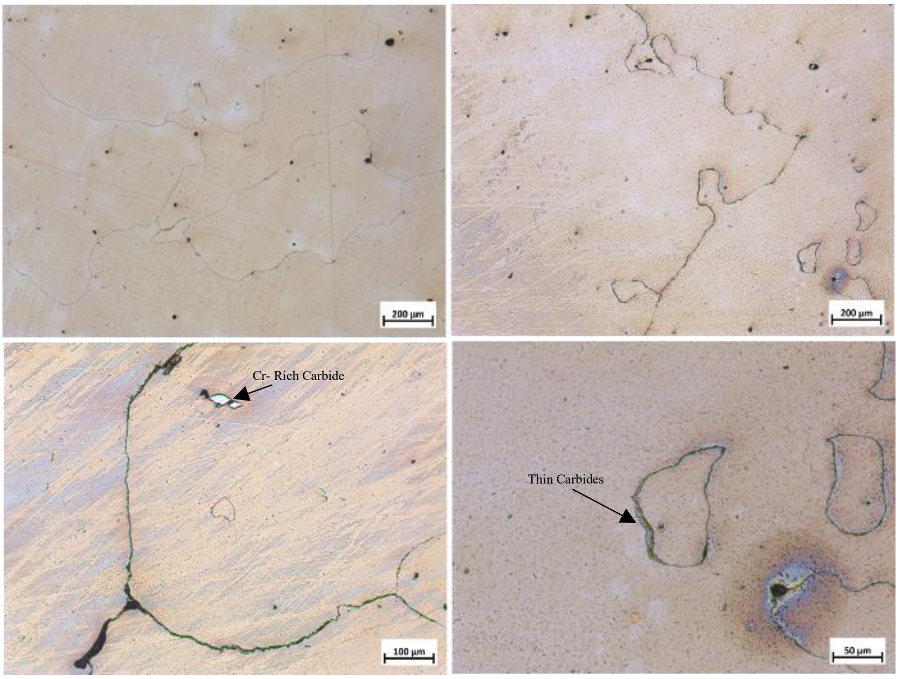

Figure 36: Grade A1-Near surface Microstructure.

- At the center of the block:

This region represents the core of the block, where the effective soaking time is lowest and the cooling rate during quenching is the slowest.

The microstructure shows an austenitic matrix containing thicker carbides both along the grain boundaries and within the grains, compared to the other samples. Clusters of Complex carbides are observed, with varying contrasts (dark, grey and bright) suggesting the presence of multiple phases carbides. These features are most likely composed of a combination of Ti-rich carbides and re-precipitated alloy carbides. The presence of clustered inclusions can act as stress concentration sites and reduces the impact toughness of the material.

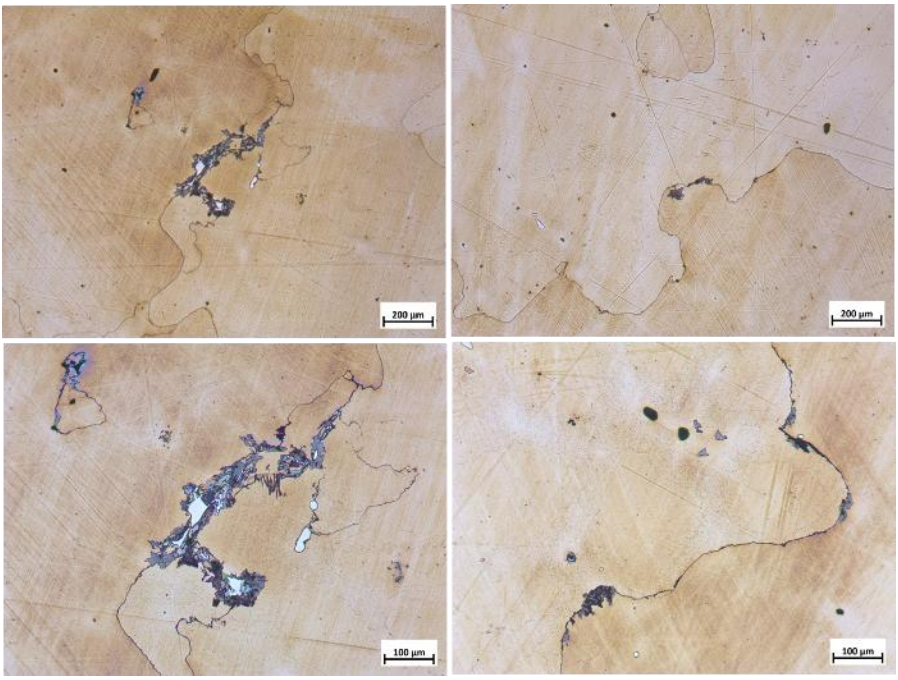

Figure 37:Grade A1-Core Microstructure.

The differences in the microstructure observed between the edge, near-surface, and core samples clearly highlight the challenges associated with heat treating Hadfield steel components with large section thickness. These results support the need for considering section-thickness limitations when designing components and optimizing heat-treatment procedures.

III. HT5- X (GRADE A5)

Heat treatment 5 represents a two-steps heat treatment process designed to refine grain sizes by promoting a temporary pearlitic formation initially at intermediate temperature and then reaching the austenitization temperature to retain austenite and dissolve carbides.

The grade A5 microstructure consists of a fully austenitic matrix with significantly finer grains compared with the as cast condition. No carbide precipitation is observed either along the grain boundaries or within grains, which indicates that the Heat treatment method was successful in achieving both objectives: carbides dissolution and grain refinement.

As shown in Figure 38, different spherical dark features are presented in the sample, which represented most likely gas porosities.

Additionally, agglomerations of small particles are presented within the microstructure, which seems most likely as Titanium Nitrides (TiN), due to their appearance, however, it needs to be confirmed using SEM/EDS.

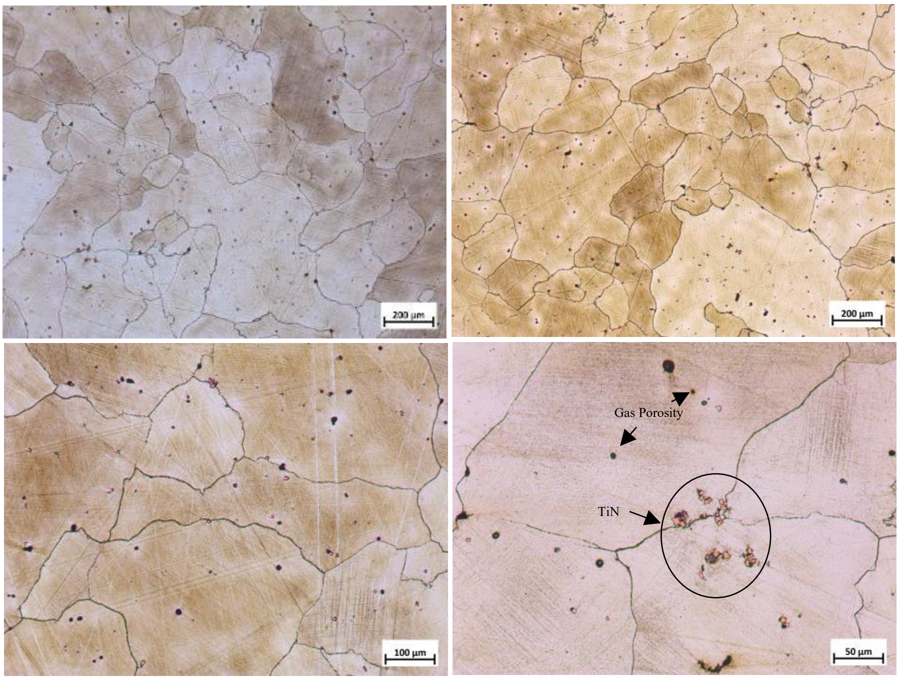

Figure 38: Grade A5 Microstructure.

4.2.2. Grade B:

The grade B manganese steel includes several conditions, starting with as-cast state.:

I. As Cast Grade B

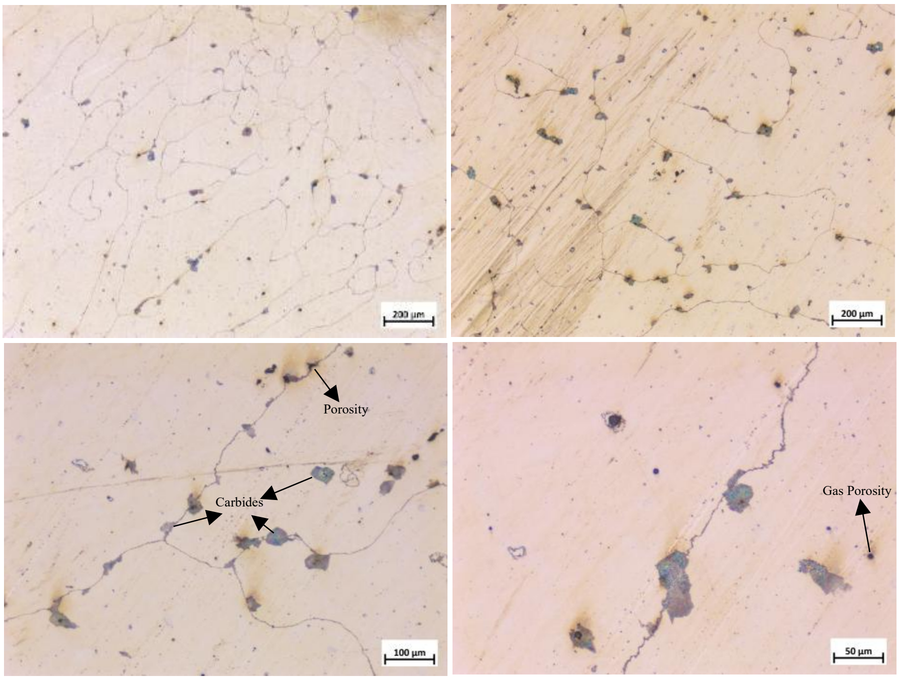

Figure 39: As Cast grade B Microstructure

The as-cast grade B microstructure shows a high level of carbide precipitation both along grain boundaries and within grain. In addition, a relatively fine grain structure is observed, which indicates the effectiveness of grain refining elements.

Several particles are observed precipitating along grain boundaries and within grains. These particles are most likely alloyed Carbides formed due elements segregation during solidification. Several dark irregular and rounded features are observed which represents most likely casting-related porosities.

II. HT1- Y (GRADE B1)

The same heat-treatment cycle and sampling procedure described for HT1-grade A were applied for the grade B block. Three regions were analyzed:

- At the edge of the block:

The edge represents the region in the block with the longest exposure to solution-treatment and the fastest cooling rate during quenching.

The microstructure consists of fine-grained austenitic matrix with clean grain boundaries. Carbide precipitation along grain boundaries is significantly reduced, indicating that the heat treatment was effective in

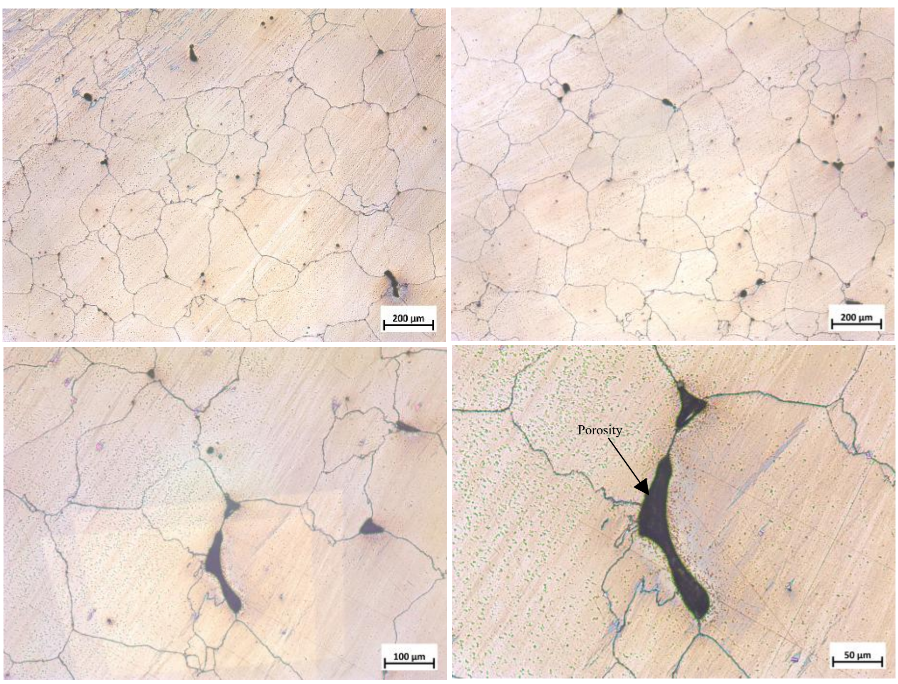

Figure 40: Grade B1-Edge Microstructure.

dissolving most of the carbides and that the rapid quenching limited carbide re-precipitation. However, casting-related porosities are observed within the microstructure.

- Near the surface of the block:

This region represents 1 inch from the edge and experienced slightly lower soaking time and a slower cooling rate compared to the sample taken from the edge.

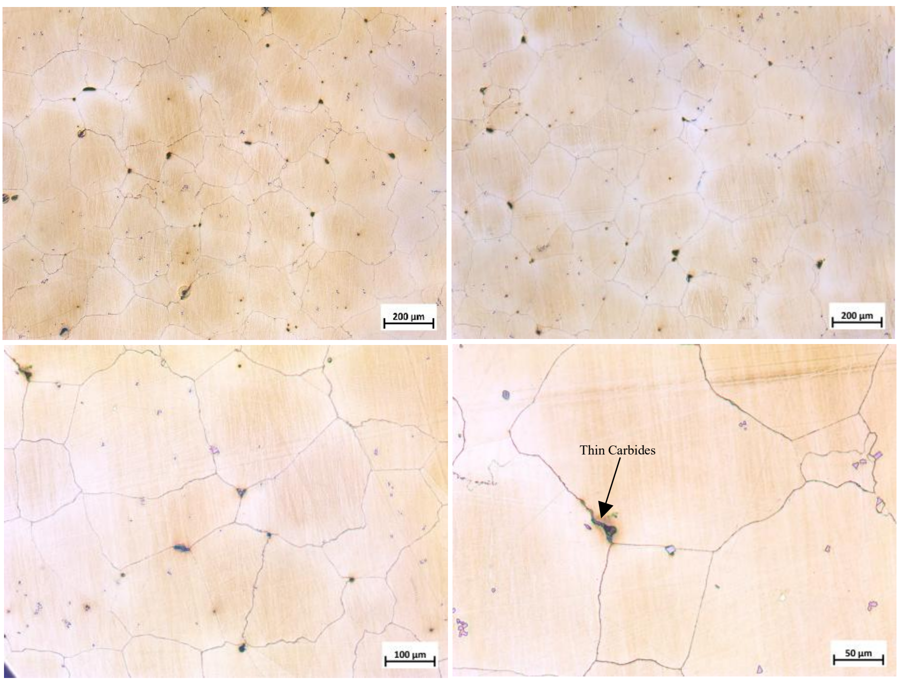

Figure 41: Grade B1- near surface Microstructure.

The microstructure consists of fine-grained austenitic matrix and with small particles along the grain boundaries; which are most likely re-precipitated carbides. Although these carbides are present, they are not continuous throughout the sample, suggesting that the heat treatment was largely effective in dissolving most of the carbides in the sample. Their limited presence is not expected to affect the mechanical performance of the material.

- At the center of the block:

This region presents the core of the block, with the lowest soaking time and slowest cooling rate during quenching.

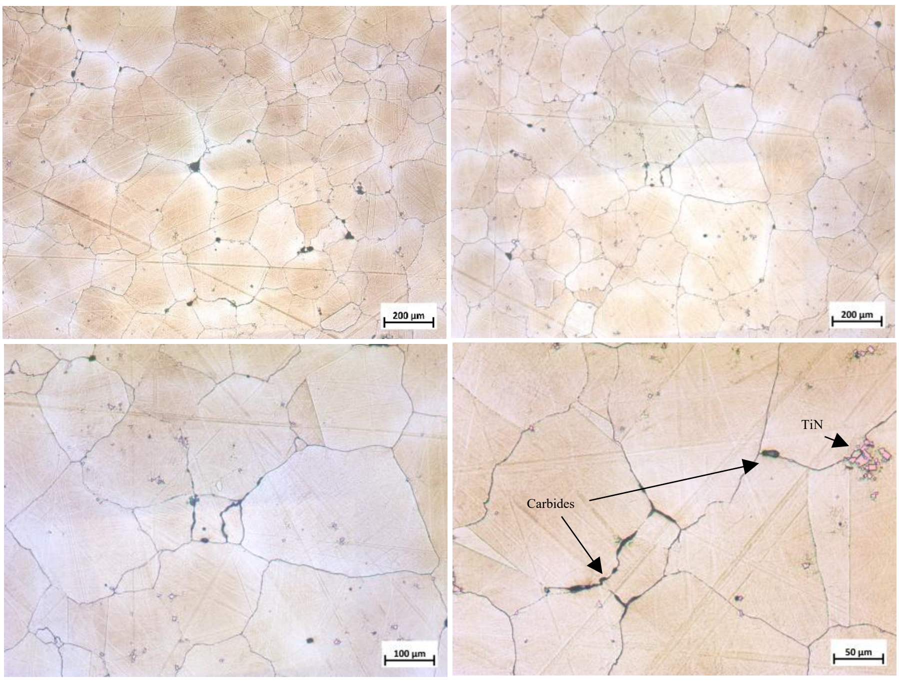

Figure 42: Grade B1-Center Microstructure.

The microstructure shows an austenitic matrix containing thicker and more continuous re-precipitated carbides along the grain boundaries compared to the edge and near-surface regions.

In addition, agglomerations of small particles are presented within the microstructure, which seems most likely as Titanium Nitrides (TiN), based on their appearance, however, it needs to be confirmed using SEM/EDS.

The difference in the microstructure between the three different regions highlights the challenge of heat-treating Hadfield steel parts with large section thickness.

A comparison between grade A and grade B samples indicates the influence of alloy composition on the microstructural response. The presence of grain-refining elements in grade B resulted in a finer grain structure. While the higher manganese content delay carbide precipitation, leading to a reduced amount of re-precipitated carbides in grade B compared to grade A.

III. HT2- Y (GRADE B2)

Heat treatment 2 represents a reference heat treatment cycle designed for small plates, followed by quenching from the austenitizing temperature. This cycle is used as a baseline for comparison with the temperature step-down heat treatment method aiming for a better quenching.

The grade B2 microstructure consists of fine-grained austenitic matrix with clean grain boundaries compared to the as-cast condition. No carbide precipitation is observed either along the grain boundaries or within grains, which indicates that this reference heat treatment method is successful in dissolving the carbides and not causing grain growth.

Compared to HT1, which had a significantly thicker sample, a more uniform carbide-free microstructure is observed. This highlights the influence of section thickness on the effectiveness of heat treatment process.

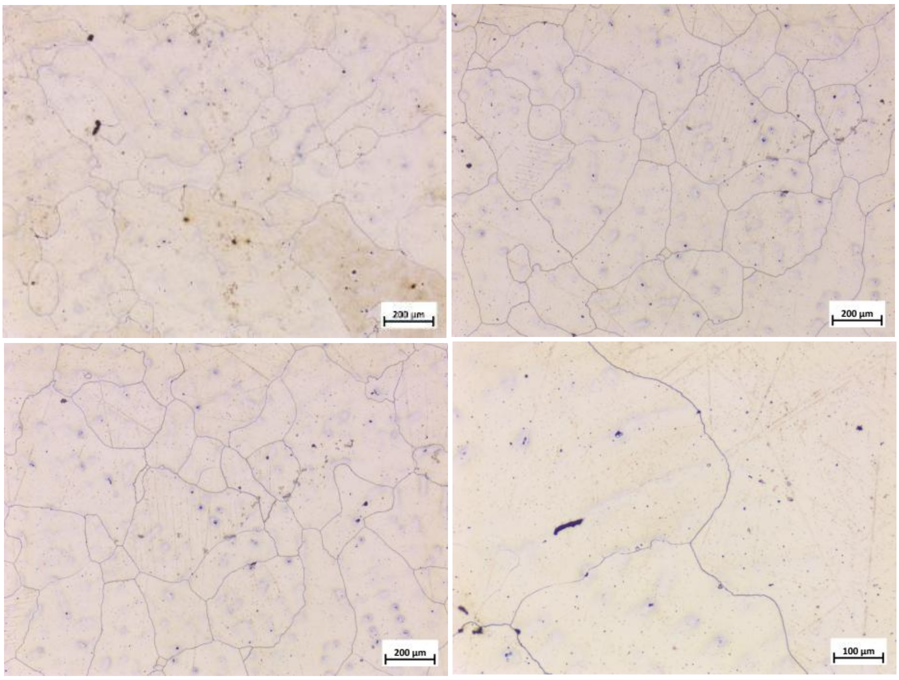

Figure 43: Grade B2 Microstructure.

IV. HT3- Y (GRADE B3)

Heat treatment 3 represents a heat-treatment cycle designed for small plates, in which the temperature is stepped down to 1000°C prior to quenching. This approach reduces the amount of heat that must be removed during quenching and is intended to shorten the quenching time.

The grade B3 microstructure consists of fine-grained austenitic matrix with clean grain boundaries, similar to the reference sample (grade B2). No carbide precipitation is observed along the grain boundaries or within grains, indicating that stepping down the temperature to 1000°C prior to quenching was successful and does not promote carbide re-precipitation and does not lead to noticeable grain growth.

The successful outcome of this heat treatment method shows strong potential for optimizing industrial heat treatment cycles. This approach may be particularly more beneficial for thicker components, were quenching times vary significantly between different regions of the part, as observed in the thermocouple experiment.

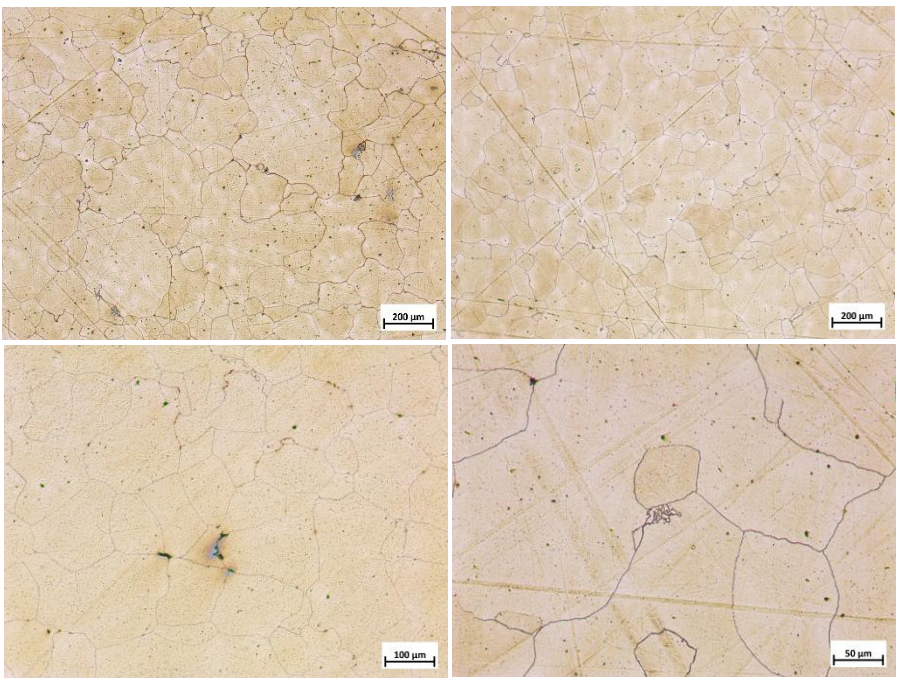

Figure 44: Grade B3 Microstructure.

However, further investigations on thicker test samples are required before applying this method industrial production.

V. HT4- Y (GRADE B4)

Heat treatment 4 represents a heat-treatment cycle designed for small plates, in which the temperature is stepped down to 900°C prior to quenching. This approach reduces the amount of heat that must be removed during quenching and is intended to shorten the quenching time.

The grade B4 microstructure consists of austenitic matrix containing fine carbides, in contrast to the reference sample (grade B2).

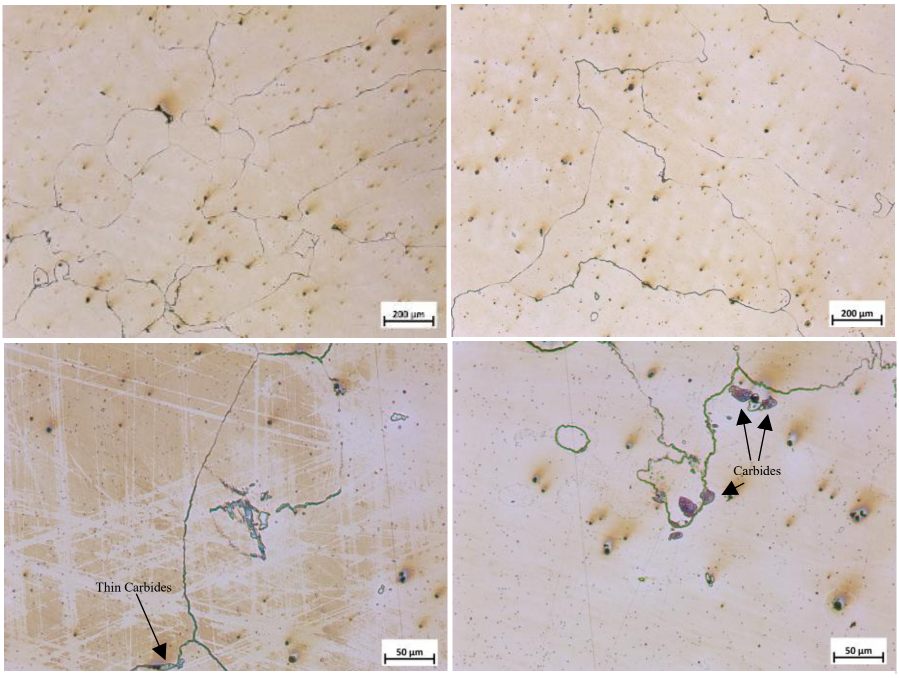

Figure 45: Grade B4 Microstructure.

Carbide re-precipitation is observed both along the grain boundaries and within grains, indicating that stepping down the temperature to 900°C prior to quenching was not successful. It also led to noticeable grain growth, which suggests that the longer heat exposure the sample faced during the step-down phase to reach 900°C, did cause grain coarsening.

The failure of this heat treatment method which caused carbide re-precipitation is most likely because of the temperature loss during the transfer of the sample from the furnace to the quenching bath. Due to lower starting temperature of the part at the point when taking out of the furnace, the sample likely entered the carbide re-precipitation temperature region before the actual quenching started.

VI. HT5- Y (GRADE B5)

Heat treatment 5 represents a two-steps heat treatment process designed to refine grain sizes by promoting a temporary pearlitic formation initially at intermediate temperature and then reaching the austenitization temperature to retain austenite and dissolve carbides.

The grade B5 microstructure consists of a relatively coarser-grained austenitic matrix containing fine carbides, compared to the reference sample (grade B2). Thin carbide precipitation is observed along the grain boundaries, which indicates that this Heat treatment method was not successful in achieving both objectives of complete carbides dissolution and grain refinement.

The difference in response between the grade A and grade B to this HT method is most likely due to their variation in chemical composition. This two-step heat treatment method was originally designed for conventional Hadfield steel with chemical composition similar to the grade A. The higher alloying content in grade B alters the transformation behaviour during the intermediate holding stage at 700°C. At this temperature range carbides formation occur but eventually pearlite starts forming after a certain amount of time, this kinetics are most likely different between the two steel grades.

As a result, the applied holding time and temperature may not be sufficient to achieve the intended purpose of this HT method in the grade B. Nevertheless, the presence of such thin carbides is unlikely to affect the mechanical performance of the material due to their limited presence.

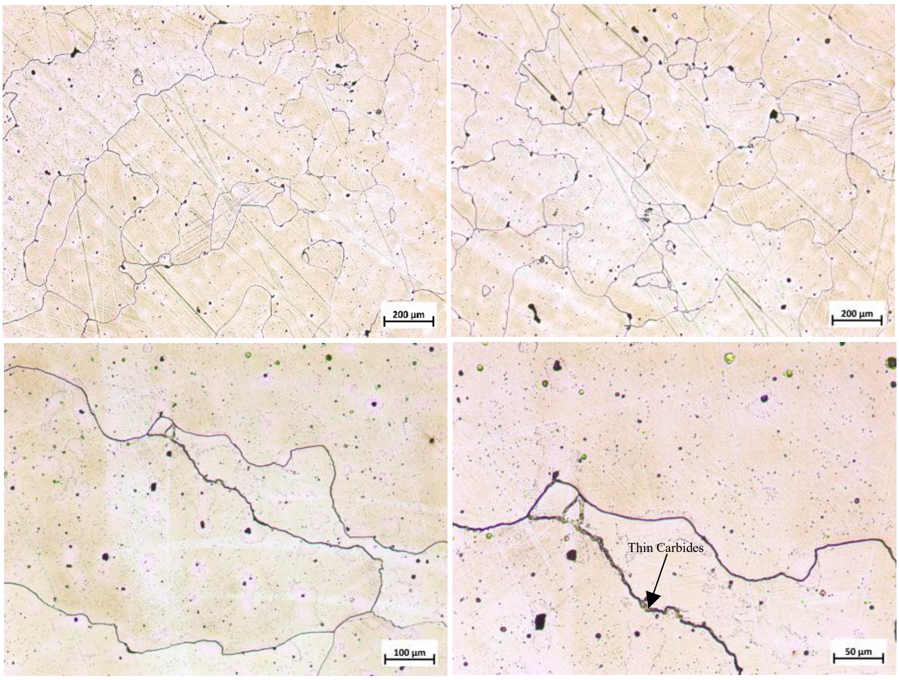

Figure 46: Grade B5 Microstructure.

4.3. Grain size

Average grain sizes were calculated using the linear intercept method on three images for each sample in order to examine the microstructural changes of the different steel grade and to evaluate the effects of the various heat treatment cycles on grain sizes.

The average grain size values are shown in figure 47.

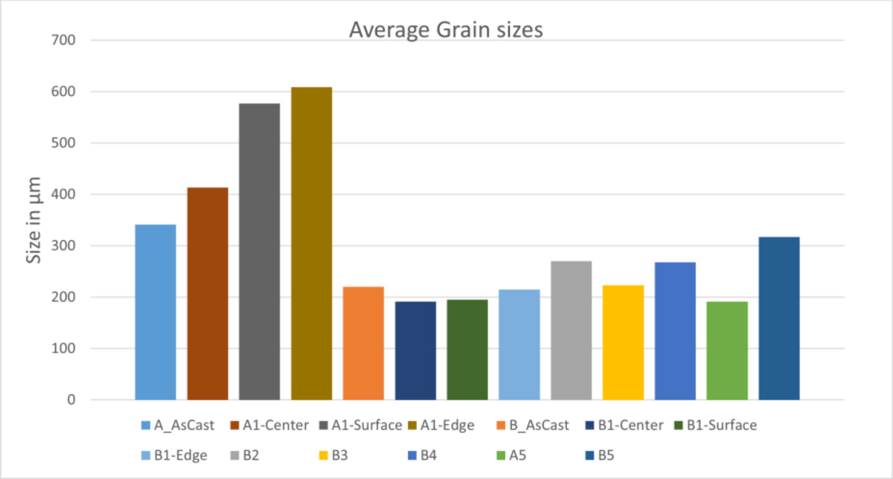

Figure 47: Average grain size values.

In the as-Cast condition, the grade A has a relatively coarse grain (~310 µm), where the grade B had a finer grain structure (~200 µm). This difference is due to the use of grain refining element in grade B, which act as nucleation sites during solidification and limit grain growth.

In the HT1 condition (thick section samples), a significant increase in grain size is observed in the grade A sample, especially in the samples taken from the edge and near surface regions. This highlights the effect of grain growth due to the longer soaking time at high temperature. In contrast, the present of carbide in the core region sample appears to restrict grain growth. On the other hand, the grade B sample shows a similar grain structure across all regions, with only minor variations in grain sizes. This confirms the effectiveness of grain-refining addition in limiting grain coursing.

In the thin section of grade B plates (HT2-HT4), the reference cycle (HT2) showed a relatively small grain growth (~270 µm) compared to the as-cast sample. In HT3, the grain growth is further limited, resulting in a finer grain structure (~230 µm), this indicates that this method effectively limits grain coarsening. In contrast, HT4 has a grain size of (~270µm) similar to the reference cycle, this was mostly due to the longer thermal exposure the sample faced during the step-down phase to reach 900°C, which led to grain coarsening.

The two step heat treatment cycle (HT5) shows different behaviour depending on the steel grade. In grade A, the method successfully refines the grain size (~190µm), confirming its effectiveness on conventional Hadfield steel. However, in grade B, the same method did cause grain growth to (~320µm) and had the largest grain sizes across all the grade B samples. This difference behaviour is mostly due to variation in the chemical composition between the two grades, as the method was originally developed for conventional Hadfield steel that have similar composition to grade A.

Overall, the results highlights that the grain size is strongly affected by both heat treatment parameters and chemical composition. It should be noted that, due to the lack of time in this project, the measurement was performed on only three images per sample, which resulted high standard deviation values. Therefore, additional measurement on larger number of images and samples from different regions are recommended to validate the obtained results.

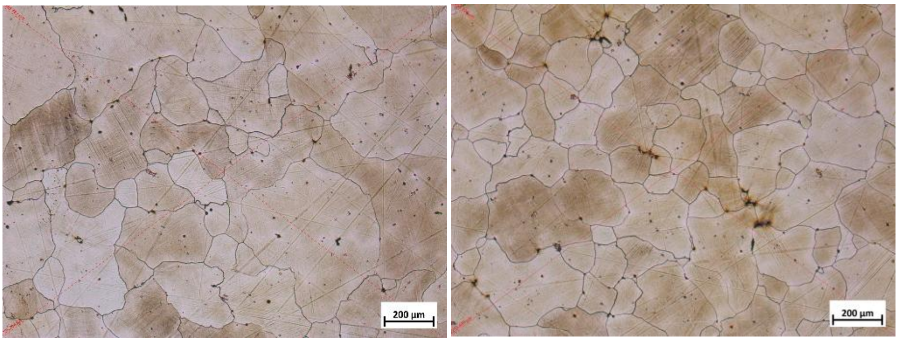

Figure 48: Grain size measurements examples.

4.4. Vickers Hardness Analysis

Microhardness Vickers tests were performed using a using 4x2 indentation matrix on each sample to calculate the average hardness values. These measurements were used to examine the changes in the mechanical performance of the different steel Grades and to evaluate the effects of the various heat treatment cycles on the material hardness.

The average hardness values for all samples are shown in figure 49.

In the as-Cast condition, the grade A shows a higher hardness (~310 HV), compared to the grade B (~220 HV). This difference is mainly due to the higher presence of carbides in the grade A microstructure in compared to the finer structure in the grade B.

In the HT1 condition (thick section samples), grade A shows an increase in the hardness toward the core, reaching the highest values (~380 HV). This behaviour is associated with the incomplete carbide dissolution and slower cooling rates in the core region. In contrast, the grade B shows a lower hardness in the core region (~270 HV) compared to the edge of the sample (~320 HV). This opposite trend can be linked to the higher manganese content in the grade B, which delays carbide re-precipitation and reduces the severity of quenching. As a result, the hardness variation in grade B is probably more influenced by chemical segregation rather than carbide distribution as in the grade A.

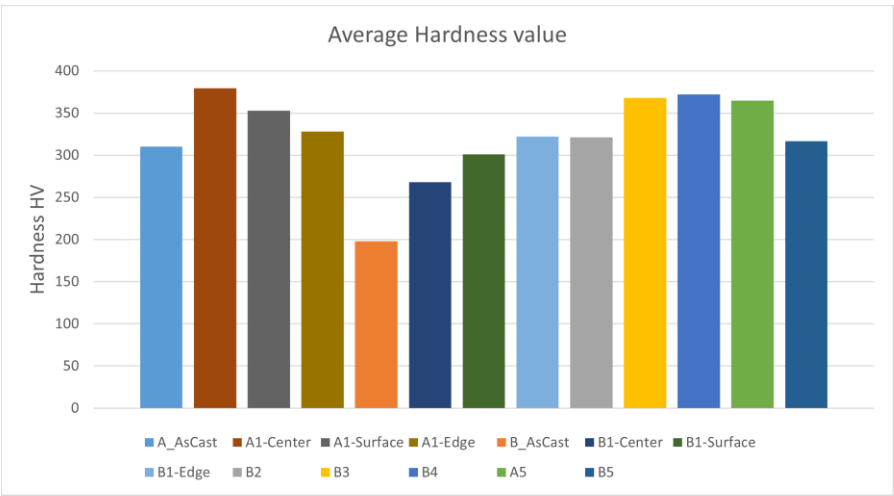

Figure 49: Average HV values.

In the thin section of grade B plates (HT2-HT4), a clear trend is observed. The reference cycle (HT2) showed a moderate hardness value (~320 HV). In HT3, hardness increases to (~360 HV), while maintaining carbide-free microstructure. This suggests that the increase in hardness may be from the formation of micro-thin carbides that increases the strength and the hardness of the steel without affecting its toughness. In HT4, the hardness is further increases (~370 HV) which is correlated to the presence of re-precipitated carbides observed in the microstructural analysis.

The HT5 cycle shows similar behaviour in both steel grades. In grade A, the method results in a higher hardness (~360 HV) compared to as-cast condition, while in grade B, the hardness increases to (~310 HV) compared to the as-cast condition.

Overall, the results highlights that the hardness is mostly linked to carbide content and chemical composition. It should be noted that, due to the lack of time in this project, the hardness tests were performed on only one sample per heat treatment condition. Therefore, additional measurement on multiple samples from different regions are recommended to further validate the obtained results.

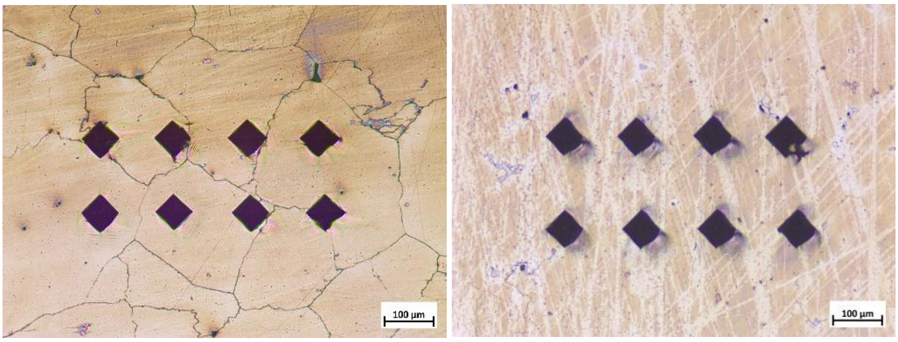

Figure 50: Hardness measurements examples.

5. Conclusion

This thesis investigated different heat treatment cycles and their effects on carbide dissolution, grain size, and hardness in different Hadfield steel alloys. In addition, K-type thermocouples were placed at different depths to monitor the temperature homogeneity, temperature evolution, and capture the thermal gradients between the surface and core regions of thick components during heat treatment and quenching.

Based on the results obtained, the main conclusions of this thesis are as follows:

- The addition of grain-refining elements had a clear influence on the grain size. Grade B showed a finer grain structure compared to Grade A in both as-cast and heat-treated conditions. This finer structure could potentially improve the toughness of the material.
- The different chemical composition of the two steel grades affected the obtained microstructure in some heat treatment cycles, especially in relation to grain growth and carbide re-precipitation.
- During the heating stage, the thermal gradient between the surface and core regions was relatively small, approximately 20-50°C on average. This indicates that the current heating rate of 100-200°C/h is sufficient for the investigated block geometry. The results also suggest that increasing the heating rate to 200-300°C/h could potentially reduce the ramping-up stage from 6 hours to 5 hours, without increasing the risk of thermal cracking.

- During quenching, the thermal gradient between the surface and core was much higher, approximately 200-400°C on average. The near surface regions cooled much faster than the core, and the core required approximately twice as long to cool down. This indicates that quenching, rather than heating, is the main limitation in the heat treatment process for thick-section Hadfield steel components.
- The heating and cooling curves of both steel heat treatments showed similar trends and values. This indicates that section thickness had a larger influence on the effectiveness of heat treatment than the chemical composition.
- Stepping down the temperature to 1000°C before quenching showed promising results. This method reduced the amount of heat that had to be removed during quenching, thus shortening the quenching time. The method succeeded in achieving carbide-free microstructure, without affecting grain size. Therefore, this heat treatment method has potential for optimizing the quenching process, especially for thicker components. However, further experiments on thick-section samples are required before applying this method in production.
- The two step heat treatment cycle was successful for the grade A sample, where it refined the grain size and dissolved carbides effectively. This indicates strong potential for improving the toughness of grade A. However, the same method was not successful for grade B, where it led to grain coarsening and carbide precipitation. This behavior is most likely related to the higher

alloying content in grade B, which altered the transformation behavior during the first holding stage.

6. References

[1] H. S. P. a. K. Applications, ”MetalZenith,” [Online]. Available: https://metalzenith.com/blogs/steel-properties/hadfield-steel-properties-and-key-applications. [Använd 10 3 2026].

[2] G. Tweedale, ”The metallurgist as entrepreneur: The career of Sir Robert Hadfield,” *Historical Metallurgy,,* vol. 26, nr 2022, pp. 19-30, 2022.

[3] Jafarian, H.R. and Sabzi, M. and Mousavi Anijdan, S.H. and Eivani, A.R. and Park, N., ”The influence of austenitization temperature on microstructural developments, mechanical properties, fracture mode and wear mechanism of Hadfield high manganese steel,” *Journal of Materials Research and Technology,* vol. 10, pp. 819-831, 2021.

[4] B. S. Kumar, ”Simulation Optimization using Reliable Material data and Experimental substantiation on Solidification behavior of Hadfield Steel : MAGMA Simulation of Manganese Steel Wear parts for Sandvik Rock Crushers,” Jönkoping University, 2017.

[5] M. Sabzi and M. Farzam, ”Hadfield manganese austenitic steel: a review of manufacturing processes and properties,” *Materials Research Express,* vol. 6, p. 1065c2, 2019.

[6] A. International, ”Standard Specification for Steel Castings, Austenitic Manganese,” A128/A128M, 2017.

[7] Faisal Qayyum, Muhammad Umar, Julia Dölling, Sergey Guk, Ulrich Prahl, ”Comprehensive Mechanics of Materials,” i *3.03 - Mechanics of New-Generation Metals and Alloys*, Elsevier, 2024, pp. 31-57.

[8] Bańkowski, Damian & Młynarczyk, Piotr & Depczyński, Wojciech & Bolanowski, Kazimierz., ”The Effect of Work Hardening on the Structure and Hardness of Hadfield Steel,” Archives of Foundry Engineering, 2024.

[9] CALPHAD, ”Thermophysical properties and structure of liquid Fe-C alloys - ,” Scientific Figure on ResearchGate, 2006. [Online]. Available: https://www.researchgate.net/figure/Fe-C-phase-diagram-CALPHADcom_fig2_286710318 . [Använd 2026].

[10] A. I. H. Committee, ”ASM Handbook, vol.3: Alloy Phase Diagrams,” ASM International, 1992.

[11] C. Chaxel, ”Investigation of Heat Treatment and Quenching Cycles on Microstructure and Mechanical Properties of Hadfield Steel,” Luleå University of Technology, 2022.

[12] Vishwajit Vishnu Kolekar, Rahul Milind Kulkarni, ”Different Heat Treatment parameters investigation on microstructure, mechanical and wear properties of Hadfield Steel,” Lund University , 2021.

[13] Zellagui, Rihab & Hemmouche, Larbi & Ait Sadi, Hassiba & Chelli, ”Effect of Element Addition, Microstructure Characteristics, Mechanical Properties, Machining and Welding Processes of the Hadfield Austenitic Manganese Steel.,” *Archives of Metallurgy and Materials.,* pp. 863-868, 2022.

[14] G. Tęcza, A. Garbacz-Klempka, ”Microstructure of Cast High-Manganese,” *De Gruyter : Archives of Foundry Engineering,* 2016.

[15] Ayadi, S., Hadji, A., ”Effect of Chemical Composition and Heat Treatments on the Microstructure and Wear Behavior of Manganese Steel.,” *Inter Metalcast 15,* p. 510–519, 2011.

[16] D. Havel, ”Austenitic Manganese Steel - A Complete overview,” Columbia Steel Casting Co, 2017.

[17] B. Lv, F.C. Zhang∗, M. Li, R.J. Hou, L.H. Qian, T.S. Wang, ”Effects of phosphorus and sulfur on the thermoplasticity of high manganese,” *Materials Science and Engineering: A,* vol. 527, nr 21-22, pp. 5648-5653, 2010.

[18] G. Tęcza, R. Zapała, ”Changes in impact strength and abrasive wear resistance of cast high manganese steel due to the formation of primary titanium carbides.,” *Archives of Foundry Engineering,* vol. 18, pp. 119-122, 2018.

[19] Saeed Kahrobaee, Ehsan Jahantigh Fard, ”Characterization of Hadfield Steels Subjected to Various Heat-Treating Processes by Nondestructive Eddy Current Method,” *Russian Journal of Nondestructive Testing,* vol. Vol.56, nr 2, pp. 151-160, 2020.

[20] O. Chikova, N. Sinitsin, V. Vyukhin, D. Chezganov, ”Microheterogeneity and crystallization conditions of Fe-Mn melts,” *Journal of Crystal Growth,* vol. 527, 2019.

[21] S. Kuyucak, P. Newcombe, P. Bruno, R. Grozdanich, and G. Looney, ”QUENCH TIME MEASUREMENT AS A PROCESS CONTROL TOOL,” CANMET, Heat treating progress., 2005.

[22] S. Kuyucak, R. Zavadil, and V. Gertsman, ”Heat-treatment Processing of Austenitic Manganese Steels,” CANMET, 2004.

[23] N. Mahomed, ”Shrinkage Porosity in Steel Sand Castings: Formation, Classification and Inspection,” intechopen, 2020.

[24] G. Santamaria, ”Heat Treatment of Austenitic Manganese Steel,” Lund University , 2003.

[25] H. R. Jafarian, M. Sabzi, S. H. Mousavi Anijdan, A. R. Eivani, and N. Park, ”The influence of austenitization temperature on microstructural developments, mechanical properties, fracture mode and wear mechanism of Hadfield high manganese steel,” *Journal of Materials Research and Technology,* vol. 10, p. pp. 819–831, 2021.

[26] Wahyudi, H., Pratiwi, S., Supriyanto, A., & Aji, D., ”The influence of heat rate and austenitization temperature on microstructure and hardness of Hadfield steel.,” *SINERGI,* vol. 27, pp. 241-248, 2023.

[27] S. Mishra and R. Dalai, ”A comparative study on the different heat-treatment techniques applied to high manganese steel,” *Materials Today: Proceedings, Elsevier Ltd,* p. 2517–2520, 2021.

[28] H., Shabnam & L., Mohammadbagher, ”Optimization of Heat Treatment to Obtain Desired Mechanical Properties of High Carbon Hadfield Steels,” *World Applied Sciences Journal,* vol. 15, pp. 1421-1424, 2011.

[29] Ham, Youn-Soo & Kim, Jeong-Tae & Kwak, Si-Young & Choi, Jeong-Kil & Yoon, Woo-Young., ”Critical cooling rate on carbide precipitation during quenching of austenitic manganese steel,” *China foundry,* vol. 7, pp. 178-182, 2010.

[30] A. Vukosavljević, A. Sedmak, S. Tadić, S. Perković i N. Radović, ”The Effect of Composition and Heat Treatment on Impact Toughness of Hadfield Steel.,” *Tehnički vjesnik,* vol. 32, nr 6, pp. 2217-2222, 2025.